Dynamics of antimicrobial resistance and virulence of *Salmonella enterica* serovar Dublin

Cheryll M Sia[1,2*], Rebecca L Ambrose[3], Mary Valcanis[2], Patiyan Andersson[2], Susan A Ballard[2], Benjamin P Howden[1,2], Deborah A Williamson[4#], Jaclyn S Pearson[3,5,6*#], Danielle J Ingle [1*#]

[1] *Department of Microbiology and Immunology, The University of Melbourne at The Peter Doherty Institute for Infection and Immunity, Melbourne, 3000, Victoria, Australia.*

[2] *Microbiological Diagnostic Unit Public Health Laboratory, Department of Microbiology & Immunology, The University of Melbourne at The Peter Doherty Institute for Infection and Immunity, Melbourne, 3000, Victoria, Australia.*

[3] *Centre for Innate Immunity and Infectious Diseases, Hudson Institute of Medical Research, Clayton, 3168, Victoria, Australia.*

[4] *Department of Infectious Diseases, The University of Melbourne at the Peter Doherty Institute for Infection and Immunity, Melbourne, 3000, Victoria, Australia.*

[5] *Department of Microbiology, Monash University, Clayton, 3168, Victoria, Australia.*

[6] *School of Medicine, University of St Andrews, St Andrews, KY16 9TF, Fife, United Kingdom.*

 # Contributed equally

*** Corresponding author**

CMS: cmsia@unimelb.edu.au

JSP: jp287@st-andrews.ac.uk

DJI: danielle.ingle@unimelb.edu.au

ABSTRACT

Salmonella Dublin is a host-adapted, invasive non-typhoidal *Salmonella* (iNTS) serovar that causes bloodstream infections in humans and demonstrates increasing prevalence of antimicrobial resistance (AMR). Here, we characterised a global population of 1,303 *S*. Dublin isolates for resistance and virulence mechanisms using a combined approach of *in silico* and *in vitro* analyses. We observed distinct populations of Vi antigen-negative *S.* Dublin circulating in different geographical regions, with the emergence of a North American cluster ~60 years ago. Further, we identified two distinct lineages in Australia, within which we discovered a novel hybrid plasmid encoding both AMR and mercuric resistance, highlighting the potential for emerging virulent and resistant lineages. These differences, in addition to the lack of Vi flagella represent adaptation mechanisms that may enhance survival and pathogenicity, and in turn affect prevention and control strategies for future *S.* Dublin infections. Collectively, our study embodies one of the most comprehensive investigations of *S*. Dublin and highlights the potential impact of pathogen adaptation on global health and economic burdens experienced by different sectors including livestock and human health.

Funding

DAW was supported by a National Health and Medical Research Council (NHMRC) Investigator Grant (GNT1174555) and a Medical Research Future Fund (MRFF) Grant (FSPGN000045). BPH is supported by NHMRC Investigator Grant (GNT1196103). DJI is supported by an NHMRC Investigator Grant (GNT1195210). JSP was supported by a Sylvia and Charles Viertel Senior Medical Fellowship. MDU PHL is funded by the Victorian Government, Australia. No conflict of interest declared.

Keywords

Invasive nontyphoidal *Salmonella*, antimicrobial resistance, heavy metal resistance, virulence; One Health

INTRODUCTION

Invasive nontyphoidal *Salmonella* (iNTS) infections are a major cause of global morbidity and mortality (1). Of the >2,500 NTS serovars, iNTS infections are associated with a relatively limited number of serovars. These include *Salmonella enterica* serovar Dublin (*S.* Dublin), *S.* Panama, *S.* Virchow, *S.* Choleraesuis and *S.* Typhimurium ST313 (2–4). *S.* Dublin, a bovine-adapted pathogen, is one of the leading iNTS serovars both in Australia and globally (5–7), and is associated with bacteraemia in a high proportion of infections (2,5–7). Symptomatic cattle may develop septicaemia and transplacental transmission (7,8), while asymptomatic infections in cattle enable persistence within the herd population, facilitating disease spread (7,9). *S.* Dublin causes zoonotic infections predominately through the consumption of contaminated dairy and meat produce (10–12), and as such is considered a 'One Health' pathogen. (10–12).

Antimicrobial resistance (AMR) in NTS has increased over the past several decades, leading to the reduction of therapeutic options (6,13). Although *S.* Dublin isolates are largely susceptible to therapeutics, AMR has become increasingly prevalent in *S.* Dublin (7,12,14–16). For example, a multidrug-resistant (MDR; defined as resistance to ≥ 3 antimicrobial classes (17)) lineage has recently been described in North America, characterised by varying profiles of AMR to ampicillin, streptomycin, chloramphenicol, sulphonamides, tetracyclines and third generation cephalosporins. These MDR *S.* Dublin isolates all type as sequence type 10 (ST10), and the AMR determinants have been demonstrated to be carried on an IncC plasmid that has recombined with a virulence plasmid encoding the *spvRABCD* operon with IncX1 and IncFII replicons, to produce a 329kb megaplasmid (12,16).

76

77 *S.* Dublin is closely related to *S.* Enteritidis and *S.* Gallinarum (18), with differences in
78 accessory genome content reflective of adaptation to different ecological niches (18). The
79 majority of the STs reported for *S.* Dublin are ST10 or single-locus variants of this ST, although
80 there is a second lineage, ST74, that is distinct from the main *S.* Dublin population (19). This
81 uncommon *S.* Dublin lineage, ST74, may be variably serotyped as *S.* Dublin or *S.* Enteritidis
82 dependent upon the strains used to generate typing sera in different laboratories (19), which
83 may have also contributed to it not being identified. The antigenic formula of *S.* Dublin
84 (1,9,12:g,p:-) is highly similar to *S.* Enteritidis (1,9,12:g,m:-), with three non-synonymous
85 point mutations in *fliC* (Ala220Val, Thr315Ilc and Thr318Ala) differentiating the two serovars.
86 Although the Vi flagella antigen (encoded by the *viaB* locus) is part of the antigenic definition
87 for *S*. Dublin, it has been shown that the Vi antigen is absent in many *S.* Dublin isolates (19,20).
88 Other putative virulence determinants in *S.* Dublin include *Salmonella* pathogenicity islands
89 (SPIs) 6 and 19, which both encode type VI secretion system (T6SS) machineries (21,22). The
90 presence of two T6SSs in *S*. Dublin contrasts with other NTS serovars, which encode a single
91 T6SS (21,22). T6SSs are molecular nanomachines that deliver effector proteins into eukaryotic
92 and/or prokaryotic cells to promote pathogen survival within multispecies and complex
93 immune environments such as the gut. Recent studies have demonstrated a role for SPI-6 and
94 SPI-19 in interbacterial competition by specific *S.* Dublin strains (23,24), however their effect
95 on host immune processes remains largely unknown.

96

97 We previously undertook a genomic investigation of another emerging NTS lineage in
98 Australia, *Salmonella enterica* serovar 4,[5],12:i:-, and identified several bacterial traits that
99 may have contributed to the successful spread of this lineage (25–29). In particular, we
100 hypothesised that flagellin deletion and MDR status may have contributed to host immune

evasion and positive selection, respectively, in *Salmonella enterica* serovar 4,[5],12:i:- (30). Here, we sought to understand the contribution of virulence and resistance to the recent emergence of MDR *S*. Dublin. We interrogated a global dataset of 1,303 isolates collected from 13 countries on five continents and identified distinct geographical lineages associated with specific AMR and virulence profiles, including a lineage unique with increased capability for intracellular survival and immune evasion in human macrophages.

RESULTS

Distinct S. Dublin populations circulate globally

A total of 1,303 *S*. Dublin genomes were included in our analysis, spanning four decades (Figure 1A, Supplementary Table 1-2). This dataset included 53 genomes from humans in Australia, and 1,250 genomes from Africa, Europe, North and South America collected from humans (*n*=462), animals (*n*=551), food (*n*=223) and other sources that were not stated (*n*=67) (Figure 1B, Supplementary Table 1). In total, 1,235 genomes (99.4%) were ST10 and 58 were a single locus variant (SLV) of ST10, with two double locus variant genomes (e.g. ST4100) restricted to isolates from South America. The exceptions were ST74 and SLV ST1545 that were only detected in Australia (Figure 1C-E, Supplementary Table 3). All isolates, including the ST74 lineage, were serotyped *in silico* as *S.* Dublin. However, the ST74 lineage and a single ST10 isolate had codon profiles in *fliC* of Gly60, Leu138, Ala220, Thr315 and Ala318, in contrast to the remaining ST10 and SLV, which both had a profile of Gly60, Leu138, Val220, Ile315 and Ala318 (the previously described 'Du2' and 'Du1' electrophoretic profiles (20), respectively) (Supplementary Table 4).

A maximum likelihood (ML) phylogeny was inferred from the 1,303 genomes, revealing two major lineages of *S.* Dublin, ST74 and ST10 (Figure 1D, Supplementary Figure 1). Within the

126 ST10 lineage, five clades were identified using Bayesian Analysis of Population Structure
127 (BAPS), inferred from the alignment of 2,957 core single nucleotide polymorphisms (SNPs).
128 Four clades were broadly associated with geographical region (Supplementary Figure 1,
129 Supplementary Table 1). The Australian ST10 isolates (n = 39) clustered in clade 1, while
130 isolates from North America were associated with clade 5 (Supplementary Figure 1). The
131 BAPS clade 2 were the isolates that didn't have sufficient evidence to be split into further
132 clades, hence are spread across the tree spanning a range of geographical regions.
133
134
135 ***Emergence of S. Dublin lineages in the 20th century***
136 To investigate the emergence of *S*. Dublin clades, Bayesian phylodynamic analysis was
137 undertaken on a representative subset of 660 genomes, selected for phylogenetic, geographical
138 and AMR diversity (see methods). We inferred a maximum clade credibility (MCC) phylogeny
139 from an alignment of 3,971 SNPs using the highest supported model of a relaxed lognormal
140 molecular clock and coalescent exponential tree prior. The estimated substitution rate was 1.05
141 x 10^{-7} (95% highest posterior density (HPD): 1.16 x 10^{-7}– 9.41 x 10^{-8}), slightly higher than
142 previous estimated mean substitution rates for host-restricted *Salmonella* serovars (*S*. Typhi
143 and *S*. Paratyphi A) but lower than rates reported for host-generalist NTS serovars *S*. Kentucky
144 and *S*. Agona (31).
145
146 The topology of the MCC tree was consistent with the ML tree, with geographically associated
147 sub-clades were observed in the MCC tree (Figure 2, interactive tree is available in Microreact
148 under https://microreact.org/project/sdublinpaper). The most recent common ancestor
149 (MRCA) for the *S.* Dublin global population was inferred to be 1901 (HPD 1878-1924), with
150 the MRCA of the different clades and sub-clades largely falling between 1950 and 2000. For

151 example, the most recent common ancestor (MRCA) of clade 5 MDR isolates from North
152 America was estimated to be ~1964 (HPD 1952 -1974) (Figure 2). The MRCA of the Australian
153 sub-clade was estimated to be ~1967 (HPD 1953-1980); with the Australian and North
154 American isolates inferred to have a MRCA ~1931 (HPD 1914-1947). Moreover, three clades
155 (1, 3, and 4) had European sub-clades associated with Sweden, the UK, and Denmark,
156 respectively that were all largely susceptible to antimicrobials. Some regions, such as Europe
157 and South America, were associated with several sub-clades of *S.* Dublin, potentially
158 suggesting multiple importations and expansions, while other regions, such as Australia were
159 comprised of a single sub-clade within clade 1.
160
161 ***Resistance determinants are associated with geographical regions***
162 Different plasmid types co-occurred with different AMR and HMR determinants in the *S.*
163 Dublin population, and these were also associated with differential geographical distribution
164 (Figure 2, Supplementary Figure 3-4, Supplementary Table 1). Overall, 51.5% (667/1,295) of
165 *S.* Dublin genomes had at least one AMR determinant, with 632/667 (94.8%) isolates classified
166 as MDR. MDR *S.* Dublin was predominantly identified from North American isolates, although
167 some AMR determinants were detected in *S.* Dublin from other geographic regions (Figure 3,
168 Supplementary Figures 2-3). AMR *S.* Dublin collected from animals was common
169 (*n*=305/667; 45.7%). AMR in *S.* Dublin from food sources and humans was similar in
170 proportion (*n*=174/667; 26.1% and *n*=173/667; 25.9% respectively). Although these profiles
171 are likely impacted by the sampling frame of different studies, the source of collection was not
172 considered as a selection criterion for this study, and as such, may broadly represent the AMR
173 profiles of *S.* Dublin from different sources (Figure 3A-B, Supplementary Figure 1A-C).
174

175 The most prevalent AMR determinants were *strA-B* (*n*=620), *floR* (*n*=556), *tet*(A) (*n*=608) and
176 *sul2* (*n*=596) (Supplementary Figure 2). AMR mechanisms to ciprofloxacin (triple point
177 mutations in quinolone resistance determining regions *gyrA*[83:S-F], *gyrA*[87:D-N],
178 *parC*[80:S-I]), macrolides (*mph*(A)), and colistin (*mcr-9.1*) were each detected in single
179 genomes from *S.* Dublin clade 5 at a low frequency of 0.08% (*n*=1/1,303) in the dataset. The
180 only third generation cephalosporin (3GC) resistance mechanism detected was $bla_{\text{CMY-2}}$,
181 present in 467/667 (70%) of AMR *S.* Dublin genomes. Although *strA-B*, *tet*(A) and $bla_{\text{TEM-1}}$
182 were observed in multiple clades, *floR*, *sul2* and $bla_{\text{CMY-2}}$ were restricted to North American
183 isolates that fell in clade 5 (Supplementary Figure 2-3). This MDR profile, in addition to *strA-*
184 *strB* and *tet*(A), was mediated by IncC plasmids in 593 genomes (*n*=509 from the United States
185 of America [USA], *n*=82 and *n*=2 from the UK) (Supplementary Figure 3, 4C). Nearly all clade
186 3 isolates linked to the UK had no AMR determinants, except for four isolates collected
187 between 2010-2015 (Supplementary Figure 1-3, Figure 3, Supplementary Table 1).
188
189 In addition to AMR determinants, we characterised biocide and heavy metal resistance (HMR)
190 profiles of the *S.* Dublin isolates. Although gold resistance determinants *golS* and *golT*, were
191 ubiquitous in *S.* Dublin (*n*=1,302/1,303; 99.9%), biocide and HMR determinants generally co-
192 occurred with AMR determinants (Figure 3C, Supplementary Figures 2-3). The biocide
193 quaternary ammonium compound resistance determinant, *qacEdelta1*, was primarily identified
194 in MDR genomes from clade 5 isolates (*n*=76/614; 12.4%), associated with North America.
195 Further, HMR determinants *ter* (tellurium metal), *pcoS* (copper metal) and *arsC* (arsenate
196 metal) were detected in a single genome, SRR5905515 from North American animal isolate
197 collected in 2016, with AMR mechanisms to seven different antimicrobial classes, including
198 colistin (*mcr-9.1*) (Supplementary Figure 3, Supplementary Table 1). Mercury resistance genes
199 (*merABDEPRT*) were found in 341/614 (55.5%) MDR clade 5 genomes, while *merCPRT* genes

200 were detected in single MDR genomes from Australia and South America (Supplementary
201 Table 1). The *mer* operon co-occurred in 90.1% (*n* = 534) of the isolates mediated by the IncC
202 MDR plasmid, suggesting an association of this operon with resistance determinants
203 (Supplementary Figure 3, Supplementary Table 1).
204
205 ***Characterisation of S. Dublin plasmids and identification of a novel hybrid plasmid***
206 Both IncX1 (*n*=1269/1303; 97.4%) and IncFII(S) (*n*=1213/1303; 93.1%) plasmid replicons
207 were found at high frequency within the dataset, in line with previous findings (12). Three
208 plasmid replicons, namely IncN, IncX1 and IncFII(S), and a MOBF/MOBP relaxase, were
209 detected in one of the Australian *S*. Dublin ST10 genomes from clade 1 (AUSMDU00035676).
210 Comparative analysis revealed the AUSMDU00035676 plasmid lacked the *spv* operon and had
211 low homology to reference IncN and IncX1/IncFII(S) plasmids previously associated with
212 *Salmonella* (Supplementary Figure 5, Supplementary Table 5). The loss of the *spv* operon may
213 be associated with a less invasive phenotype (32). This finding suggests the detection of a
214 potentially novel hybrid plasmid with IncN/IncX1/IncFII(S) markers that encodes AMR and
215 HMR determinants flanked by IS26 elements, which may aid gene mobilisation (33). In
216 contrast, the AUSMDU00056868 plasmid had IncX1/IncFII(S) plasmid replicon markers and
217 was found to not encode any mechanisms for resistance. This plasmid was >99% homologous
218 to known virulence reference *S.* Dublin plasmids pOU1115 and pSDU2_USMARC_69807 and
219 encoded the *spv* operon (Supplementary Table 5, Supplementary Figure 6). This suggests that
220 the *S.* Dublin virulence plasmid is conserved, while the *spv* operon that has been shown to
221 enhance disease severity (14,16,34–36) is maintained on the plasmid.
222
223 ***Diversity in virulence determinants across S.* Dublin lineages**

224 To investigate the potential for invasiveness within *S.* Dublin, we applied a previously
225 described bioinformatic tool to our dataset of 1,303 *S.* Dublin genomes (37). In brief, this tool
226 infers the likelihood of invasiveness by assigning an index score between 0 to 1 that reflects
227 the level of genome degradation, whereby a higher score suggests genomic features that may
228 be more associated with a narrower host range and great likelihood of invasiveness (37). We
229 performed initial validation work using 36 complete publicly available reference genomes,
230 covering known invasive and non-invasive phenotypes (Supplementary Table 8). Using this
231 validation set, invasive and largely host-restricted serovars, including *S.* Choleraesuis, *S.*
232 Paratyphi and *S.* Typhi, scored >0.5, suggestive of an invasive genomic profile (Figure 4A,
233 Supplementary Table 8). Conversely, non-invasive NTS serovars with broader ecological
234 niches, including *S.* Anatum, ST19 *S.* Typhimurium and *S.* Derby, scored <0.5 (Figure 4A,
235 Supplementary Table 8). When applied to our *S.* Dublin dataset, only eleven genomes
236 (*n*=11/1,303; 0.84%) had an index score < 0.5. These included three ST10 genomes and all
237 eight ST74 genomes (Figure 4B, Supplementary Table 6). No association was observed
238 between index scores and region or source attribution (Figure 4B).
239
240 Putative virulence determinants identified in *S.* Dublin genomes included SPIs, the *spv* operon
241 (16), prophages and other individual genes (Supplementary Table 6). Some putative virulence
242 factors, such as *pagN* [cell adhesion and invasion (38,39)] and *pgtE,* [virulence (26,40)], were
243 found in 1,303 (100%, *n*=1,303/1,303) and 1,302 (99.9%, *n*=1,302/1,303) genomes
244 respectively, and no SNPs in the promoter region of *pgtE* were detected, a mutation previously
245 reported in invasive *S.* Typhimurium ST313 (26). In contrast, ST313-gi of unknown function
246 (26,40), the Gifsy-2 like prophage [unknown function (26,40)] and *ggt* gene thought to be
247 involved in gut colonisation (34), were detected in the major ST10 *S.* Dublin lineages, and
248 absent in ST74 *S.* Dublin. The *viaB* operon encoding the Vi flagella antigen was only detected

249 in SLV ST73, a historical isolate from France that displayed the Du3 electrophoretic type that
250 was consistent with a previous study (20). This suggests that the Vi antigen is not conserved in
251 the *S.* Dublin population or associated with virulence. Further, there was no association
252 between the number of virulence determinants and the AMR and HMR profile of isolates,
253 suggesting a potential lack of fitness cost associated with resistance mechanisms and virulence
254 (Supplementary Table 6).
255
256 The presence of SPI-6 and SPI-19 differed across *S.* Dublin isolates. Both SPIs encode T6SSs
257 that provide a means for injecting effector proteins into adjacent competing bacteria or host
258 cells for immune evasion (22,41). SPI-19 was absent in the ST74 *S.* Dublin lineage but present
259 in all ST10 *S.* Dublin (Supplementary Figure 7). The genetic differences between ST74 and
260 ST10 were reflected in the disparity of their index scores of <0.5 and >0.5, respectively. The
261 SPI-6 region was detected in all isolates, however <90% sequence coverage was detected in
262 422/1,303 genomes (32.4%). Long read sequencing on three genomes of the ST74 lineage and
263 three genomes from the ST10 clade 1 lineage corroborated these findings (Figure 4C-E),
264 demonstrating truncation of SPI-6 with the T6SS machinery (Figure 4D). Long-read
265 sequencing also revealed an absence of SPI-19 in the three ST74 isolates and presence of SPI-
266 19 in the three ST10 isolates (Figure 4C, E). The absence of SPI-19 in ST74 suggests that this
267 deletion event occurred during its divergence from the primary *S*. Dublin lineage, ST10.
268
269 ***Infection of human macrophages reveals distinct intracellular replication patterns between***
270 ***ST10 and ST74 lineages***
271 Given the distinct genomic profiles of ST10 and ST74 lineages, we compared the phenotypic
272 profile of a selection of Australian isolates from each lineage *in vitro*. The immortalised human
273 macrophage cell line, THP-1, was used to assess invasion, intracellular replication and host

274 cytotoxicity induced by a subset of clinical isolates from the two lineages. Specifically, we
275 assayed an ST10 population comprising eleven isolates, including an isolate from the highly
276 related ST4293 lineage, and an ST74 population comprising seven isolates including an isolate
277 from the highly related ST1545 lineage (Supplementary Table 10). Although predicted invasive
278 index scores were higher for the ST10 population (Figure 4B), each isolate failed to replicate
279 more than 2-fold over 24 hours in THP-1 cells (Figure 5A), whereas isolates within the ST74
280 population displayed a sustained increase in fold change of intracellular replication, up to 8-
281 fold, over 24 hours (Figure 5B). Comparing bacterial growth (CFU/ml) across both sequence
282 types, both lineages were comparable for initial bacterial uptake (Figure 5C) however, the ST74
283 population replicated to significantly higher levels in THP-1 macrophages at 9- and 24-hours
284 post-infection (hpi) compared to the ST10 population (Figure 5D-F). Given that NTS also
285 replicate in epithelial cells, we utilised an immortalised human intestinal epithelial cell line,
286 HT-29, to assess *S.* Dublin replication. In contrast to the results obtained in macrophages, we
287 found that 6 out of 11 isolates within the ST10 population replicated more efficiently (up to
288 10-fold) in HT-29 cells, whereas all seven isolates within the ST74 population showed minimal
289 replication (up to 2-fold) over 24 hours (Supplementary Figure 8A-C).
290

291 ***Increased replication of ST74 isolates in human macrophages does not correlate with***
292 ***increased host cell death***

293 It is well documented that protype *S.* Typhimurium (ST19) potently induce macrophage
294 cytotoxicity both *in vitro* and *in vivo* (42). Here, we utilised a cellular lactate dehydrogenase
295 (LDH) release assay to assess THP-1 cytotoxicity in response to infection with *S.* Dublin ST74
296 and ST10 populations. Surprisingly, the substantial intracellular replication of the ST74
297 population in THP-1 cells induced significantly less host cell cytotoxicity at 3 and 9 hpi
298 compared with the ST10 population suggesting potential immune evasion by ST74 (Figure 6A,

299 B). By 24 hpi however, cytotoxicity induced by both ST74 and ST10 populations was relatively
300 high, with no significant difference observed across the sequence types (Figure 6C). In contrast,
301 there was minimal cytotoxicity observed in infected HT-29 cells across the board
302 (Supplementary Figure 8D), suggesting a less potent activation of host cell death in infected
303 epithelial cells compared with macrophages.
304
305 To understand how the ST74 population may be supressing macrophage death at earlier stages
306 of infection, we measured protein secretion of IL-1ß via cytokine release and immunoblot
307 assays at 9 hpi, respectively. IL-1ß is a potent pro-inflammatory cytokine that is released upon
308 activation of the NLRC4 inflammasome by components of the *Salmonella* type III secretion
309 apparatus (43), resulting in a lytic cell death process known as pyroptosis (44). Here, we
310 observed significantly less IL-1ß release by THP-1 cells infected with isolates from the ST74
311 population at 9 hpi compared with those from the ST10 population (Figure 6D), directly
312 reflecting the LDH cytotoxicity data represented in Figure 6B. To further support our
313 observations, we selected single representative isolates of ST74 and ST10 to perform
314 immunoblot analyses of cleaved IL-1ß (activated form) within THP-1 cells. Here, ST74
315 induced less IL-1ß cleavage at 9 hpi compared to the ST10 (Figure 6E). We included the
316 ubiquitous laboratory NTS reference strain, *S.* Typhimurium SL1344 in the immunoblot
317 analysis as this is known to potently induce pyroptosis in human macrophages (45). As
318 expected, SL1344 induced significant IL-1ß cleavage during infection of THP-1 macrophages
319 (Figure 6E). To assess the correlation of cellular cytotoxicity as measured by LDH, IL-1ß
320 release and intracellular replication, we generated a PCA plot of all isolates within the ST74
321 and ST10 populations. Here we can clearly demonstrate that isolates from the ST74 population
322 have increased replicative ability, induce less cytotoxicity, and lower levels of IL-1ß release
323 (Figure 6F) compared with those within the ST10 population. There were however, some ST10

324 isolates that induced similarly low levels of host cell death, presumably due to lower levels of
325 intracellular replication (Figure 6F and Supplementary Figure 9A, B). These isolates generally
326 clustered away from the ST10 isolates that induced more cell death (Supplementary Figure
327 9C).
328
329 A pangenome analysis of the isolates from both ST10 and ST74 lineages revealed that out of a
330 total of 5,792 genes, there were 473 and 1,143 genes specific to the ST10 and ST74 lineage,
331 respectively (Supplementary Figure 10, Supplementary Table 11). Further, out of 1,143 genes,
332 there were 362 core genes present in all isolates from the ST74 lineage (Supplementary Table
333 11). While these findings require further investigation, an increased gene content and genome
334 size were consistently observed in all isolates of the ST74 lineage (Supplementary Table 9 and
335 11). These results suggest an association with unique genome content of the ST74 lineage and
336 may account for altered host responses and replicative ability (Supplementary Table 9).
337
338 **DISCUSSION**
339 Our data provide comprehensive insights into the emergence and spread of distinct lineages of
340 *S*. Dublin, with striking geographic associations with AMR and virulence, consistent with
341 previous work (12). Analysing the largest global dataset of *S*. Dublin genomes to date, we show
342 that highly resistant *S.* Dublin is almost entirely confined to North America, with emergence in
343 the late 20th century and ongoing local microevolution. North American *S.* Dublin isolates in
344 clade 5 were characterised by the presence of an IncC plasmid, often with co-location of AMR
345 and heavy metal resistance determinants. Heavy metals and biocides are both used in the agri-
346 food industry and may contribute to the persistence of AMR via co-selection (46). The co-
347 occurrence of AMR, HMR and biocide resistance determinants in animal, food and human *S.*
348 Dublin genomes highlights the potential for selection pressure in one ecological niche (e.g. the

349 use of biocides in farming or heavy metals in animal feeds) leading to AMR in another (e.g.
350 AMR in humans).
351
352 The phylogeographic separation of *S.* Dublin lineages is consistent with other studies (7,12,47),
353 and is likely to be influenced by several factors, including local AMR use and patterns of
354 livestock movement. Given the livestock reservoir of *S.* Dublin is relatively host-restricted to
355 cattle, it is conceivable that both historic and contemporary global cattle movement may have
356 contributed to region-specific differences in *S.* Dublin. For example, Australian *S.* Dublin
357 genomes in clade 1 shared a common ancestor with North American isolates in clade 5. During
358 the early 1930's, Brahman cattle were imported from the U.S into Australia (48), supporting
359 our phylodynamic finding that the common ancestral link between *S*. Dublin isolates from
360 North America and Australia emerged in the early-mid 20th century. Following region-specific
361 introductions, it is likely that local antimicrobial and husbandry practices may then contribute
362 to the local evolution of *S.* Dublin. In contrast to North American MDR isolates, ST10 *S.*
363 Dublin isolates from Australia were predominantly fully susceptible to antimicrobials.
364 Selective pressure, misdirected treatment, the misuse of antimicrobials in cattle and MDR
365 plasmids in agricultural settings have been associated with the increase of MDR *S*. Dublin cases
366 in North America (49). Conversely, the use of antimicrobials has been extensively minimised
367 in the Australian dairy industry, hence cattle infections are rarely associated with AMR (50).
368 Consistent with regional differences in AMR profiles were geographic differences in plasmid
369 profiles. IncC plasmids are large (70-250kb), can encode up to 10 AMR determinants and are
370 widespread in North America (51–53), while IncN plasmids are smaller (30-70kb), encode up
371 to seven AMR determinants and are widespread in Europe (51,53,54).
372

373 Of note, amongst *S.* Dublin isolates from Australia, genomic analysis (cf. serotyping) revealed
374 a smaller population of ST74 isolates. *S.* Dublin ST74 was previously identified as *S.*
375 Enteritidis ST74, and sits as an intermediate between *S*. Dublin and *S*. Enteritidis (19), and has
376 been understudied to date in studies of *S.* Dublin. The difference between the antigenic formula
377 of *S*. Dublin and *S*. Enteritidis is in the H1 flagella region, which is typed as "*g,p*" for *S.* Dublin
378 and "*g,m*" for *S.* Enteritidis. ST74 *S.* Dublin genomes were characterised by: (i) a lack of any
379 AMR or HMR determinants; (ii) lack of complete SPI-6 regions, specifically the T6SS, and
380 (iii) a lack of putative virulence determinants including ST313-gi, Gifsy-2 like prophage and
381 SPI-19 (which encodes a T6SS mechanism for intestinal colonisation and survival that interacts
382 with the host by mediating macrophage cytotoxicity (55)). Our data demonstrated that while
383 machine learning predicted the ST74 population to have a lower potential for invasiveness
384 compared to ST10, the genetic differences in ST74 may contribute to increased replication in
385 human macrophages. Collectively, these findings highlight the co-circulation in Australia of
386 two *S*. Dublin populations, an ST10 and ST74 population, which may be phenotypically
387 characterised as *S.* Dublin.
388
389 The lack of the Vi antigen in 1,302/1,303 (99.9%) *S*. Dublin genomes has several implications.
390 First, the antigenic formula of *S*. Dublin, 1,9,12[Vi] may need to be reviewed if most *S.* Dublin
391 genomes lack the machinery to express the Vi flagella. These limitations with serotyping have
392 been highlighted in a previous study, suggesting a transition to a novel genotyping scheme that
393 would prevent these phenotypic discrepancies (56). Second, the Vi antigen is a vaccine target
394 for *S.* Typhi (57), and the Vi antigen has been explored as a target for *S.* Dublin (58). While
395 previous studies have noted that some *S.* Dublin genomes may be capable of producing the Vi
396 antigen (58), the genomic data from this study shows that these genomes are in the minority of
397 the *S.* Dublin population and may not be stable targets for *S.* Dublin specific vaccines.

398

399 Our phenotypic data demonstrated a striking difference in replication dynamics between ST10
400 and ST74 populations in human macrophages, whereby isolates within the ST74 population
401 replicated significantly over 24 hours compared with the rapid clearance of those within the
402 ST10 population after 9 hours of infection. The ST74 population generally induced
403 significantly less host cell death during the early-mid stages of macrophage infection,
404 supported by a limited processing and release of the pro-inflammatory cytokine IL-1ß at 9 hpi.
405 Research to date suggest that *Salmonellae* are potent activators of inflammasome activation
406 (59), however most of the data that support this theory have been generated using laboratory
407 adapted strains of *S.* Typhimurium. Our data, however, suggest that ST74 (and highly related)
408 isolates may utilise specific immune evasion mechanisms to avoid host recognition and the
409 activation of host cell death signalling pathways in phagocytes in the early stages of infection.
410 This observation is not unique to NTS. In 2015, Carden *et al.* (60) demonstrated that *S.*
411 Typhimurium ST313, a major cause of bacteraemia in humans in sub-Saharan Africa, induced
412 significantly less inflammasome activation compared with *S.* Typhimurium ST19 isolates
413 during infection of murine bone marrow-derived macrophages. Such events could potentially
414 facilitate increased pathogen replication and dissemination in the host at later stages of
415 infection. Indeed, we observed similarly high levels of host cell cytotoxicity in response to
416 ST10, ST74 and related isolates at 24 hpi, indicating that ST74 likely induce cell death via
417 alternative mechanisms once intracellular bacterial levels become unsustainable within the
418 macrophage. Further investigation is required to identify and validate specific genomic factors
419 that may contribute to the mechanisms of enhanced host cell survival, in particular inhibition
420 of inflammasome activation and subsequent IL-1ß release during infection with ST74 isolates.
421 Indeed, a pangenome analysis of the ST10 and ST74 lineages included in phenotypic assays
422 have revealed multiple SPI and non-SPI-related genes that are unique to the ST74 lineage

423 (Supplementary Figure 11), >900 of which remain uncharacterised. A systematic analysis of
424 these unique genes, including comparison with other invasive NTS serovars, protein function
425 prediction and targeted mutagenesis may reveal genes of interest that contribute to pathogen
426 survival in the hostile immune environment of a macrophage.
427
428 To date, SPI-19 has been identified in NTS serovars Dublin, Weltevreden, Agona, Gallinarum
429 and Enteritidis (22), however the lack of SPI-19 in the *S.* Dublin ST74 lineage (Figure 4C and
430 E, Supplementary Figure 7, Supplementary Table 6) is an interesting observation and may
431 suggest a specific adaptation that supports increased replicative ability in phagocytes. In
432 previous studies, *S.* Dublin SPI-19 has been associated with colonisation and manipulation of
433 intestinal microbiome in poultry (21,55), as well as contributing to oral (but not systemic)
434 virulence in mice (55). Collectively, these outcomes suggest a role for SPI-19 at the mucosal-
435 luminal interface of the intestinal tract, possibly contributing to colonisation of intestinal
436 epithelial cells. Given that ST74 isolates replicate so efficiently in macrophages, it may be that
437 they simply do not require the added benefit of SPI-19-mediated mucosal colonisation and rely
438 solely on their ability to access phagocytes via M cell or dendritic cell uptake at the apical
439 surface of the intestine. The fact that ST74 isolates have a much larger pangenome than ST10
440 isolates, may also contribute to successful colonisation, replication and survival within the host
441 and thus compensate for the lack of SPI-19 function. Regardless, this work highlights how little
442 we know about the specific host-pathogen interactions of NTS and what specifically drives the
443 success of potential emerging lineages of iNTS.
444
445 This study has both strengths and limitations. It represents the most comprehensive genomic
446 study of *S.* Dublin to date, systematically characterising antimicrobial, heavy metal and biocide
447 resistance determinants, in addition to exploring the virulome in the global population of *S.*

448 Dublin. Importantly, our phenotypic data reveals the caution required when making generalised
449 statements about infection outcomes and virulence mechanisms of *Salmonella* serovars. Our
450 data clearly shows that within the Dublin serovar, there are distinct phenotypic differences
451 observed across sequence types and host cell types, all of which could impact significantly on
452 future development of effective therapeutics or vaccine strategies for NTS infections. The key
453 limitation of this dataset is the geographical distribution bias with an overrepresentation of
454 North American genomes and the lack of data from other regions, such as Asia. However, this
455 is a common limitation of many genomic studies and often results in a bias towards high
456 income countries that have greater resources for whole genome sequencing. This situation may
457 change in the future as many countries build their public health genomics capacity.
458
459 In conclusion, we provide genomic insights into the evolutionary, resistance and virulence
460 dynamics in *S.* Dublin circulating globally. The increasing incidence of iNTS caused by *S.*
461 Dublin may warrant this pathogen becoming a notifiable disease, similar to typhoid and
462 paratyphoid fever. The distinct virulence and AMR profiles of *S.* Dublin globally warrant
463 revisitation of the current classification scheme for NTS, in keeping with the rapid and ongoing
464 evolution of these significant pathogens. Importantly, our data further highlight the need for a
465 One Health approach to genomic surveillance.
466
467
468 **METHODS**
469
470 ***Setting and dataset***
471 For Australian isolates, whole genome sequencing (WGS) was performed on all viable *S.*
472 Dublin isolates from human clinical samples received at the Microbiological Diagnostic Unit

473 Public Health Laboratory (MDU PHL), the primary bacterial reference laboratory for the State
474 of Victoria in Australia. In total, 53 *S*. Dublin genomes between 2000-2019 were included. For
475 publicly available data, we included *S*. Dublin sequences that had associated metadata
476 (geographical origin and date of sample collection), providing a total of 1,250 publicly
477 available sequences. Data were collected in accordance with the Victorian Public Health and
478 Wellbeing Act 2008. Ethical approval was received from the University of Melbourne Human
479 Research Ethics Committee (study number 1954615.3).
480
481 ***Genome quality control, assembly and serovar prediction***
482 Genomes were assembled and quality controlled using the Nullarbor pipeline v2.0.20191013
483 (https://github.com/tseemann/nullarbor). Briefly, Skesa v2.4.0 (61) was used to assemble the
484 genomes before determining the sequence type (ST) using the multilocus sequence typing
485 (MLST) scheme '*senterica'* within mlst v2.19.0 (https://github.com/tseemann/mlst). Kraken
486 v1.1.1 (62) was then used to confirm the taxonomic classification. Snippy v4.6.0
487 (https://github.com/tseemann/snippy) with parameters set to a 0.90 variant rate proportion
488 against a minimum coverage of 10X mapped the reads against a well-studied reference
489 genome, *S*. Dublin CT_02021853 (NC_011205.1). To be included in subsequent analysis,
490 genomes had to pass the following quality control parameters: mapped to ≥ 80% of the
491 reference genome; had a ≥ 80% taxonomic sequence similarity to *S. enterica*; N50 >25000,
492 and <300 contigs. To verify that each genome was *S*. Dublin, all sequences were typed using
493 *Salmonella* in silico Typing Resource (SISTR) v1.1.1 (63). The electrophoretic type of each
494 isolate was determined using Antimicrobial Resistance Identification by Assembly (ARIBA)
495 v2.14.5 (64) against the reference Du 2 (Genbank accession: M84972.1).
496
497 ***Core genome phylogenomic analysis***

498 Variant calls from snippy were used to construct a core genome single nucleotide
499 polymorphism (SNP) alignment using snippy-core v4.6.0
500 (https://github.com/tseemann/snippy). Phaster v2020-12-22 (65) was used to create a BED file
501 containing prophage regions. The option '—mask' in snippy-core was used to exclude the
502 identified prophage regions from the BED file. Constant sites from the reference genome were
503 obtained using the script iqtree-calc_const_sites.sh (https://github.com/MDU-PHL/mdu-
504 tools/blob/master/bin/iqtree-calc_const_sites.sh). A maximum-likelihood (ML) phylogeny was
505 inferred using IQ-TREE v2.1.0 (66) with parameters set to a GTR+G4 nucleotide substitution
506 model with constant sites and ultrafast bootstrapping (67) to 1000 replicates. The resulting ML
507 tree was then visualised using *ggtree* v2.3.3 R package (68). Population clades were defined
508 using rhierBAPS v1.1.3 to one level on an alignment of 2,957 core SNPS of 1,295 isolates in
509 the ST10 *S.* Dublin lineage (69)
510
511 ***In silico prediction of resistance determinants and plasmid replicons***
512 To screen for quinolone point mutations and acquired AMR determinants, ARIBA and
513 AbriTAMR v0.2.2 (https://github.com/MDU-PHL/abritamr) were used, respectively. The
514 AMR database used for this study was the NCBI AMRFinderPlus database v2020-01-22.1.
515 Each isolate's susceptibility profile was classified as either susceptible; resistant to 1-2
516 antimicrobials, or multidrug resistant (MDR). Heavy metal and biocide determinants were
517 identified by screening the AMRFinder database v2020-07-16.2 with AMRFinder v3.8.4 (70).
518 Replicon types were determined using ABRicate v1.0.1 (https://github.com/tseemann/abricate)
519 at a threshold of 80% nucleotide identity and 95% coverage, and screening against the
520 Plasmidfinder database (71). A strict threshold was applied to ensure the detection of only
521 unambiguous replicon types. To establish the most common resistant profiles, co-occurrence
522 matrices of resistant determinants were constructed in R using *igraph* v1.2.4.1 (72).

523

524 ***Virulome analysis***

525 Virulence genes were identified using ABRicate at 90% nucleotide identity/coverage against
526 the virulence factor database (vfdb) v2018-03-18 (73). Databases from previous studies
527 (16,26,34,74–78) were also interrogated and collated. This included a database containing
528 additional virulent determinants and *Salmonella* pathogenicity islands (SPIs) -1, -2, -6 and -19
529 (Supplementary Table 7). Using ABRicate, the presence of SPIs -1, -2, -6 and -19 were
530 identified at 80% ID and 10% COV. ABRicate was also used to screen the manually created
531 SPI determinant database for genes relevant to SPI-1, -2, -6 and -19 with a threshold of 90%
532 identity/coverage (Supplementary Table 7). To quantify invasiveness, index scores were
533 calculated *in silico* for each isolate using Wheeler *et al.*'s tool developed in 2018 for inferring
534 the likelihood of invasiveness (http://www.github.com/UCanCompBio/invasive_*Salmonella*),
535 with a higher score for an isolate deemed more invasive (37). Prior to running the tool, a set of
536 reference genomes consisting of invasive and non-invasive *Salmonella* serovars were used as
537 a validation set (Supplementary Table 8). The validation results were then visualised using
538 *ggtree*.

539

540 ***Bayesian phylodynamic analysis***

541 A subset of 660 *S*. Dublin genomes from the main cluster was used for BEAST v1.10.4 (79)
542 analysis. This subset comprised all Australian genomes and a proportion of international *S*.
543 Dublin genomes. The sampling strategy for selecting representative international genomes
544 involved capturing all geographical regions and sources harbouring distinct susceptibility
545 profiles. When two genomes demonstrated the same AMR profile and were from the same
546 region and source, the oldest genome was preferred. Recombination sites were filtered using
547 Gubbins v2.4.1 (80). A core genome SNP alignment of these genomes was created using

548 snippy-core v4.6.0 and then a ML phylogeny was inferred as above. Temporal signal was
549 assessed using TempEst v1.5.3 (81) by assessing the best-fitting root using the heuristic
550 residual mean squared method. The core alignment was then used to create an xml file in
551 BEAUti v1.10.4 using the GTR+G4 substitution model. To identify the most appropriate model
552 for our dataset, a combination of using either a "relaxed lognormal" or a "strict" molecular
553 clock with either a "coalescent constant" or a "coalescent exponential" population prior was
554 tested. For all models, the Markov chain Monte Carlo chain length was set to 300,000,000 and
555 sampling was set to every 20,000 trees with the marginal likelihood estimation set to
556 "generalised stepping stone (GSS)" to provide statistical support. The analysis was repeated in
557 triplicates with and without tip dates to ensure there was no temporal bias. Bayesian evaluation
558 of temporal signal (BETS) was used to determine whether a temporal signal was present (82).
559 To optimise computational resource and time, BEAST v1.10.4 was used with BEAGLE v3.0.2
560 (83). A Maximum Clade Credibility (MCC) tree from the highest supported model using GSS
561 was extracted using TreeAnnotator v1.10.4 and median heights. The resulting MCC tree was
562 then visualised using *ggtree*.
563
564 ***Long read sequencing***
565 The Oxford Nanopore Technologies MinION platform was used to obtain complete genomes
566 of six Australian *S.* Dublin genomes (Supplementary Table 9). These genomes, comprised of
567 ST10 lineage clade 1 (AUSMDU00056868 and AUSMDU00035676,) and ST74
568 (AUSMDU00016676 and AUSMDU00021231), were selected based on their AMR profile,
569 virulome and index scores. To prepare new DNA libraries for long read sequencing, genomes
570 were freshly re-cultured. DNA was extracted using the Virus/Pathogen DSP midi kit on the
571 QiaSymphony SP instrument. Sequencing libraries were prepared using a Ligation sequencing
572 kit (SQK-LSK109) with native barcode expansion and sequenced for 48 hours on a GridION

573 Mk2 instrument using a R9.4 flowcell. WGS was performed using the Illumina NextSeq
574 500/550 platform (Illumina, San Diego, CA). Demultiplexed long reads and corresponding
575 WGS reads were subjected to QC to exclude unreliable reads using fastp v0.20.1 (84) and
576 Filtlong v0.2.1 (https://github.com/rrwick/Filtlong), respectively. Long reads were assembled
577 using Trycycler v0.4.1 (85). The final sequence was polished using Medaka v1.4.3
578 (https://github.com/nanoporetech/medaka). To ensure small plasmids were not excluded during
579 the initial QC step, hybrid assemblies using both long and WGS reads were generated
580 Unicycler v0.4.4 (86). Trycycler assemblies were checked against Unicycler assemblies with
581 Bandage v0.8.1 (87). The final genome assemblies were confirmed as *S*. Dublin using SISTR
582 and annotated using Prokka v1.14.6 (88) (Supplementary Table 9).
583
584 Chromosomal assemblies were aligned to complete genomes of known *S*. Dublin references
585 CT_02021853 (CP001144.1, without Vi flagella) and CFSAN000518 (CP074226.1, with Vi
586 flagella) and visualised using Blast Ring Image Generator (BRIG) v0.95 (89). Plasmid
587 assemblies were screened using PlasmidFinder (90) and mob-typer v3.1.0 (91) to identify
588 replicon and relaxase types, respectively. Plasmid profiles were subjected to BLASTn against
589 previously identified IncX1/IncFII(S) virulence plasmids reported in *S.* Dublin and IncN
590 plasmids associated with serovars of *Salmonella* (Supplementary Table 5). Genome
591 comparisons of plasmids demonstrating the top four highest BLASTn max scores were
592 visualised using BRIG. Prokka was used to annotate the regions of interest, while Easyfig
593 v2.2.2 (92) was used to compare regions of the genome. Regions of the genome were
594 visualised using the R package *gggenomes* v0.9.12.9000
595 (https://github.com/thackl/gggenomes).
596
597 ***Human cell line infections***

598 Human macrophage (THP-1) (ATCC® TIB-202™) and colonic epithelial (HT-29) (ATCC®
599 HTB-38™) cell lines were maintained in Roswell Park Memorial Institute (RPMI) 1640 media
600 + 200 mM GlutaMAX (Life Technologies) supplemented with 10% v/v Fetal Bovine Serum
601 (FBS; Bovogen) and grown in a humidified 5% CO2 37ºC incubator. THP-1 monocytes were
602 differentiated into macrophages with 50 ng/mL phorbol 12-myristiate-12 acetate (PMA,
603 Sigma-Aldrich) for 72 hours prior to infection.
604
605 Single colonies of each *S*. Dublin isolate were inoculated into 10 mL Luria Bertani (LB) broth
606 and grown overnight at 37ºC at 200 rpm, then sub-cultured for 3 hours in the same conditions
607 in 5 mL LB. Colony forming units/mL were measured by absorbance at 600 nM (OD_{600}). THP-
608 1 and HT-29 cells were infected at a multiplicity of infection (MOI) of 10 in RPMI in triplicate
609 wells of a 96-well plate and centrifuged at 525 x g for 5 minutes to synchronize bacterial
610 uptake. Infected cells were incubated at 37ºC for 30 minutes, then infective media removed
611 and replaced with 100 µg/mL gentamicin in 10% v/v FBS/RPMI to inhibit extracellular
612 bacterial growth. 0 hours post infection (hpi) samples were collected at this time to measure
613 initial bacterial uptake. Cells were then incubated in high dose gentamicin for 1 hour, then
614 replaced with 10 µg/mL gentamicin in 10% v/v FBS/RPMI for the remainder of the infection.
615 For THP-1 cells, samples were collected at time 0-, 3-, 9- and 24-hours post-infection. For HT-
616 29 cells, samples were collected at 0- and 24-hours post-infection.
617
618 Cytotoxicity of infection was measured by lactate dehydrogenase (LDH) release by infected
619 cells before lysis for intracellular bacterial enumeration. Briefly, 35 uL of infected (and
620 uninfected) cell culture supernatants were collected from each well and LDH quantified as per
621 manufacturer's instructions (Promega), with percent cytotoxicity calculated as a proportion of
622 lysed control cells and blank media. Following this, infected cells were washed three times

623 with warm phosphate-buffered saline (PBS) to remove any lingering extracellular bacteria,
624 then lysed in 0.1% Triton X-100/PBS and plated out onto LB agar after serial dilution. Bacterial
625 enumeration and cell viability assays were performed over 3 biological replicates, each
626 performed independently, with a new passage of host cells, on a separate day. Within each
627 biological replicate, technical triplicates were performed for each isolate. All statistical
628 analyses were performed using Prism software (GraphPad Software v9.0) and determined by
629 nested students t-test, which allowed for inclusion of individual isolates in sub-groups of each
630 sequence type (ST10 vs ST74).
631
632 ***Measurement of cellular responses***
633 THP-1 cells were infected at an MOI of 10 with a representative isolate from each of the ST10
634 and ST74 lineages as described above, then lysed in radio-immunoprecipitation (RIPA) buffer
635 (20 mM Tris pH 8.0, 0.5 mM EDTA, 150 mM NaCl, 1% v/v Triton X-100, 0.5% w/v sodium
636 deoxycholate, 0.1% w/v SDS) supplemented with Complete protease and phosphatase inhibitor
637 cocktails (Roche) at 0-, 3-, 8- and 24 hpi . Total protein concentration was quantified by
638 Bicinchoninic acid (BCA) assay and 15 µg separated on 4-12% Bolt Bis-Tris polyacrylamide
639 gels (Thermo Scientific), transferred to nitrocellulose (iBlot, Thermo Scientific) and blotted
640 for cleaved IL-1β (clone D3A3Z, Cell Signalling). Cell culture supernatants were also collected
641 from 96-well plate infections at 9 hpi and secreted IL-1β measured by DuoSet© Human IL-
642 1β/IL-1F2 ELISA as per manufacturer's instructions (R&D Systems). A core genome SNP ML
643 phylogeny was constructed on the Australian ST10 lineage to demonstrate the genetic
644 relationship of representative ST10 isolates that underwent *in vitro* phenotypic assays.
645
646 ***Pangenome analysis***

647 The pangenomes of the isolates used in the macrophages and epithelial infections were
648 analysed using Panaroo v1.3.4 (93) set to default threshold settings, under strict mode and with
649 the removal of invalid genes on the draft genome assemblies (Supplementary Table 11).
650

651 **DATA AVAILABILITY**

652 Paired end reads of public data were obtained from either the European Nucleotide Archive
653 (ENA) or National Center for Biotechnology Information (NCBI). The Australian short read
654 data and complete genomes for the four Australian *S.* Dublin isolates are available at the NCBI
655 Sequence Read Archive under BioProject PRJNA319593. Details of all 1,303 genomes
656 included in the study are available in Supplementary Tables 1-11. These supplementary tables
657 also includes *i*) the resistance, virulence, Vi and *fliC* profiles of all 1,303 genomes; *ii*) the
658 genbank accession numbers of all reference genomes, virulence determinants and IncN
659 plasmids used in this study, and *iii*) all raw CFU, cytotoxicity and ELISA values from the
660 phenotypic analyses. The interactive tree is available in Microreact under
661 https://microreact.org/project/sdublinpaper).
662

663 **CODE AVAILABILITY**

664 The machine learning tool developed by Wheeler *et al*. for predicting the likelihood of
665 invasiveness is available in a public Github depository
666 http://www.github.com/UCanCompBio/invasive_*Salmonella*.
667

668 **REFERENCES**

669 1. Stanaway JD, Parisi A, Sarkar K, Blacker BF, Reiner RC, Hay SI, et al. The Global
670 Burden of Non-typhoidal *Salmonella* Invasive Disease: A Systematic Analysis for the
671 Global Burden of Disease Study 2017. The Lancet Infectious Diseases.
672 2019;19(12):1312–24.

673 2. Parisi A, Crump JA, Stafford R, Glass K, Howden BP, Kirk MD. Increasing incidence of
674 invasive nontyphoidal *Salmonella* infections in Queensland, Australia, 2007-2016. PLOS
675 Neglected Tropical Diseases. 2019 Mar 18;13(3):e0007187.

676 3. Mughini-Gras L, Pijnacker R, Duijster J, Heck M, Wit B, Veldman K, et al. Changing
677 Epidemiology of Invasive Non-typhoid *Salmonella* Infection: A Nationwide Population-
678 based Registry Study. Clinical Microbiology and Infection. 2020;26(7):941.e9-941.e14.

679 4. Kingsley RA, Msefula CL, Thomson NR, Kariuki S, Holt KE, Gordon MA, et al.
680 Epidemic Multiple Drug Resistant *Salmonella* Typhimurium Causing Invasive Disease in
681 Sub-Saharan Africa have a Distinct Genotype. Genome Res. 2009;19(12):2279–87.

682 5. Cheng RA, Eade CR, Wiedmann M. Embracing Diversity: Differences in Virulence
683 Mechanisms, Disease Severity, and Host Adaptations Contribute to the Success of
684 Nontyphoidal *Salmonella* as a Foodborne Pathogen. Front Microbiol. 2019 Jun
685 26;10:1368.

686 6. Williamson DA, Lane CR, Easton M, Valcanis M, Strachan J, Veitch MG, et al.
687 Increasing Antimicrobial Resistance in Nontyphoidal *Salmonella* Isolates in Australia
688 from 1979 to 2015. Antimicrob Agents Chemother. 2018 Jan 25;62(2). Available from:
689 https://www.ncbi.nlm.nih.gov/pmc/articles/PMC5786757/

690 7. Mangat CS, Bekal S, Avery BP, Côté G, Daignault D, Doualla-Bell F, et al. Genomic
691 Investigation of the Emergence of Invasive Multidrug-Resistant *Salmonella enterica*
692 Serovar Dublin in Humans and Animals in Canada. Antimicrobial Agents and
693 Chemotherapy. 2019 Jun 1;63(6). Available from:
694 https://aac.asm.org/content/63/6/e00108-19

695 8. Reichel MP, Wahl LC, Hill FI. Review of Diagnostic Procedures and Approaches to
696 Infectious Causes of Reproductive Failures of Cattle in Australia and New Zealand. Front
697 Vet Sci. 2018 Oct 2;5.

698 9. Kirchner M, McLaren I, Clifton-Hadley FA, Liebana E, Wales AD, Davies RH. A
699 Comparison Between Longitudinal Shedding Patterns of *Salmonella* Typhimurium and
700 *Salmonella* Dublin on Dairy Farms. Veterinary Record. 2012 Aug 25;171(8):194–194.

701 10. McDonough PL, Fogelman D, Shin SJ, Brunner MA, Lein DH. *Salmonella enterica*
702 Serotype Dublin Infection: an Emerging Infectious Disease for the Northeastern United
703 States. J Clin Microbiol. 1999 Aug;37(8):2418–27.

704 11. Davidson KE, Byrne BA, Pires AFA, Magdesian KG, Pereira RV. Antimicrobial
705 resistance trends in fecal *Salmonella* isolates from northern California dairy cattle
706 admitted to a veterinary teaching hospital, 2002-2016. PLoS One. 2018 Jun 28;13(6).
707 Available from: https://www.ncbi.nlm.nih.gov/pmc/articles/PMC6023112/

708 12. Fenske GJ, Thachil A, McDonough PL, Glaser A, Scaria J. Geography Shapes the
709 Population Genomics of *Salmonella enterica* Dublin. Genome Biol Evol. 2019 Aug
710 1;11(8):2220–31.

711 13. Sia CM, Baines SL, Valcanis M, Lee DYJ, Gonçalves da Silva A, Ballard SA, et al.
712 Genomic Diversity of Antimicrobial Resistance in Non-typhoidal *Salmonella* in Victoria,
713 Australia. Microbial Genomics. 2021;7(12):000725.

714 14. Paudyal N, Pan H, Elbediwi M, Zhou X, Peng X, Li X, et al. Characterization of
715 *Salmonella* Dublin isolated from bovine and human hosts. BMC Microbiology. 2019 Oct
716 16;19(1):226.

15. Harvey RR, Friedman CR, Crim SM, Judd M, Barrett KA, Tolar B, et al. Epidemiology of *Salmonella enterica* Serotype Dublin Infections among Humans, United States, 1968–2013 - Volume 23, Number 9—September 2017 - Emerging Infectious Diseases journal - CDC. [cited 2020 Nov 24]; Available from: https://wwwnc.cdc.gov/eid/article/23/9/17-0136_article

16. Hsu CH, Li C, Hoffmann M, McDermott P, Abbott J, Ayers S, et al. Comparative Genomic Analysis of Virulence, Antimicrobial Resistance, and Plasmid Profiles of *Salmonella* Dublin Isolated from Sick Cattle, Retail Beef, and Humans in the United States. Microbial Drug Resistance. 2019 May 31;25(8):1238–49.

17. Magiorakos AP, Srinivasan A, Carey RB, Carmeli Y, Falagas ME, Giske CG, et al. Multidrug-Resistant, Extensively Drug-resistant and Pandrug-resistant Bacteria: An International Expert Proposal for Interim Standard Definitions for Acquired Resistance. Clinical Microbiology and Infection. 2012;18(3):268–81.

18. Langridge GC, Fookes M, Connor TR, Feltwell T, Feasey N, Parsons BN, et al. Patterns of Genome Evolution that have Accompanied Host Adaptation in *Salmonella*. Proc Natl Acad Sci USA. 2015;112(3):863–8.

19. Achtman M, Wain J, Weill FX, Nair S, Zhou Z, Sangal V, et al. Multilocus Sequence Typing as a Replacement for Serotyping in *Salmonella enterica*. PLoS Pathogens. 2012;8(6):e1002776.

20. Selander RK, Smith NH, Li J, Beltran P, Ferris KE, Kopecko DJ, et al. Molecular Evolutionary Genetics of the Cattle-Adapted Serovar *Salmonella* Dublin. J Bacteriol. 1992;174(11):3587–92.

21. Pezoa D, Blondel CJ, Silva CA, Yang HJ, Andrews-Polymenis H, Santiviago CA, et al. Only One of the Two Type VI Secretion Systems Encoded in the *Salmonella enterica* Serotype Dublin Genome is Involved in Colonization of the Avian and Murine Hosts. Veterinary Research. 2014;45(1):2.

22. Blondel CJ, Jiménez JC, Contreras I, Santiviago CA. Comparative Genomic Analysis Uncovers 3 Novel Loci Encoding Type Six Secretion Systems Differentially Distributed in *Salmonella* Serotypes. BMC Genomics. 2009 Aug 4;10:354.

23. Blondel CJ, Amaya FA, Bustamante P, Santiviago CA, Pezoa D. Identification and distribution of new candidate T6SS effectors encoded in *Salmonella* Pathogenicity Island 6. Front Microbiol. 2023 Aug 17;14. Available from: https://www.frontiersin.org/journals/microbiology/articles/10.3389/fmicb.2023.1252344/full

24. Amaya FA, Blondel CJ, Barros-Infante MF, Rivera D, Moreno-Switt AI, Santiviago CA, et al. Identification of Type VI Secretion Systems Effector Proteins That Contribute to Interbacterial Competition in *Salmonella* Dublin. Frontiers in Microbiology. 2022;13. Available from: https://www.frontiersin.org/article/10.3389/fmicb.2022.811932

25. Vilela FP, Gomes CN, Paziani MH, Braz VS, Rodrigues D dos P, Costa RG, et al. Virulence traits and expression of *bstA, fliC* and *sopE2* in *Salmonella* Dublin strains

757 isolated from humans and animals in Brazil. Infection, Genetics and Evolution.
758 2020;80:104193.

759 26. Hammarlöf DL, Kröger C, Owen SV, Canals R, Lacharme-Lora L, Wenner N, et al. Role
760 of a Single Noncoding Nucleotide in the Evolution of an Epidemic African Clade of
761 *Salmonella*. Proc Natl Acad Sci U S A. 2018;115(11):E2614–23.

762 27. Herrero-Fresno A, Espinel IC, Spiegelhauer MR, Guerra PR, Andersen KW, Olsen JE.
763 The Homolog of the Gene *bstA* of the BTP1 Phage from *Salmonella enterica* Serovar
764 Typhimurium ST313 Is an Antivirulence Gene in *Salmonella enterica* Serovar Dublin.
765 Infection and Immunity. 2018;86(1).

766 28. Mohammed M, Cormican M. Whole Genome Sequencing Provides Insights into the
767 Genetic Determinants of Invasiveness in *Salmonella* Dublin. Epidemiology and Infection.
768 2016;144(11):2430–9.

769 29. De Sousa Violante M, Podeur G, Michel V, Guillier L, Radomski N, Lailler R, et al. A
770 Retrospective and Regional Approach Assessing the Genomic Diversity of *Salmonella*
771 Dublin. NAR Genom Bioinform. 2022 Jul 9;4(3):lqac047.

772 30. Ingle DJ, Ambrose RL, Baines SL, Duchene S, Gonçalves da Silva A, Lee DYJ, et al.
773 Evolutionary Dynamics of Multidrug Resistant *Salmonella enterica* serovar 4,[5],12:i:- in
774 Australia. Nature Communications. 2021;12(1):4786.

775 31. Duchêne S, Holt KE, Weill FX, Le Hello S, Hawkey J, Edwards DJ, et al. Genome-scale
776 Rates of Evolutionary Change in Bacteria. Microb Genom. 2016 Nov 30;2(11):e000094.

777 32. Silva C, Puente JL, Calva E. *Salmonella* Virulence Plasmid: Pathogenesis and Ecology.
778 Pathogens and Disease. 2017;75(6).

779 33. Harmer CJ, Hall RM. IS26 Family Members IS257 and IS1216 Also Form Cointegrates
780 by Copy-In and Targeted Conservative Routes. mSphere. 2020;5(1):811.

781 34. Mohammed M, Le Hello S, Leekitcharoenphon P, Hendriksen R. The invasome of
782 *Salmonella* Dublin as revealed by whole genome sequencing. BMC Infect Dis. 2017 Aug
783 4;17. Available from: https://www.ncbi.nlm.nih.gov/pmc/articles/PMC5544996/

784 35. Hong SF, Chiu CH, Chu C, Feng Y, Ou JT. Complete Nucleotide Sequence of a Virulence
785 Plasmid of *Salmonella enterica* Serovar Dublin and Its Phylogenetic Relationship to the
786 Virulence Plasmids of Serovars Choleraesuis, Enteritidis and Typhimurium. FEMS
787 Microbiology Letters. 2008;282(1):39–43.

788 36. Chu C, Feng Y, Chien AC, Hu S, Chu CH, Chiu CH. Evolution of Genes on the
789 *Salmonella* Virulence Plasmid Phylogeny Revealed From Sequencing of the Virulence
790 Plasmids of *S. enterica* Serotype Dublin and Comparative Analysis. Genomics.
791 2008;92(5):339–43.

792 37. Wheeler NE, Gardner PP, Barquist L. Machine Learning Identifies Signatures of Host
793 Adaptation in the Bacterial Pathogen *Salmonella enterica*. PLoS Genetics.
794 2018;14(5):e1007333.

795 38. Lambert MA, Smith SG. The PagN protein of *Salmonella enterica* Serovar Typhimurium
796 is an Adhesin and Invasin. BMC Microbiology. 2008;8(1):142.

797 39. Folkesson A, Advani A, Sukupolvi S, Pfeifer JD, Normark S, Löfdahl S. Multiple
798 Insertions of Fimbrial Operons Correlate with the Evolution of *Salmonella* Serovars
799 Responsible for Human Disease. Molecular Microbiology. 1999;33(3):612–22.

800 40. Herrero-Fresno A, Wallrodt I, Leekitcharoenphon P, Olsen JE, Aarestrup FM, Hendriksen
801 RS. The Role of the *st313-td* Gene in Virulence of *Salmonella* Typhimurium ST313.
802 PLOS ONE. 2014 Jan 3;9(1):e84566.

803 41. Sabbagh SC, Forest CG, Lepage C, Leclerc JM, Daigle F. So Similar, Yet So Different:
804 Uncovering Distinctive Features in the Genomes of *Salmonella enterica* Serovars
805 Typhimurium and Typhi. FEMS Microbiology Letters. 2010;305(1):1–13.

806 42. Chen LM, Kaniga K, Galán JE. *Salmonella* spp. are cytotoxic for cultured macrophages.
807 Molecular Microbiology. 1996;21(5):1101–15.

808 43. Miao EA, Mao DP, Yudkovsky N, Bonneau R, Lorang CG, Warren SE, et al. Innate
809 immune detection of the type III secretion apparatus through the NLRC4 inflammasome.
810 Proceedings of the National Academy of Sciences. 2010 Feb 16;107(7):3076–80.

811 44. Bergsbaken T, Fink SL, Cookson BT. Pyroptosis: host cell death and inflammation. Nat
812 Rev Microbiol. 2009 Feb;7(2):99–109.

813 45. Doerflinger M, Deng Y, Whitney P, Salvamoser R, Engel S, Kueh AJ, et al. Flexible
814 Usage and Interconnectivity of Diverse Cell Death Pathways Protect against Intracellular
815 Infection. Immunity. 2020 Sep;53(3):533-547.e7.

816 46. Cheng G, Ning J, Ahmed S, Huang J, Ullah R, An B, et al. Selection and Dissemination
817 of Antimicrobial Resistance in Agri-food Production. Antimicrob Resist Infect Control.
818 2019;8:158.

819 47. Srednik ME, Lantz K, Hicks JA, Morningstar-Shaw BR, Mackie TA, Schlater LK.
820 Antimicrobial Resistance and Genomic Characterization of *Salmonella* Dublin Isolates in
821 Cattle from the United States. PLOS ONE. 2021 Sep 21;16(9):e0249617.

822 48. O'Connell J. Australian Food Timeline. 1930 [cited 2022 Nov 11]. Australian food
823 history timeline - Brahman cattle imported. Available from:
824 https://australianfoodtimeline.com.au/brahman-cattle-imported/

825 49. Fritz HM, Pereira RV, Toohey-Kurth K, Marshall E, Tucker J, Clothier KA. *Salmonella*
826 *enterica* Serovar Dublin from Cattle in California from 1993–2019: Antimicrobial
827 Resistance Trends of Clinical Relevance. Antibiotics (Basel). 2022;11(8):1110.

828 50. Izzo M, Mohler V, House J. Antimicrobial Susceptibility of *Salmonella* Isolates
829 Recovered From Calves with Diarrhoea in Australia. Australian Veterinary Journal.
830 2011;89(10):402–8.

831 51. McMillan EA, Jackson CR, Frye JG. Transferable Plasmids of *Salmonella enterica*
832 Associated With Antibiotic Resistance Genes. Frontiers in Microbiology. 2020;11.
833 Available from: https://www.frontiersin.org/article/10.3389/fmicb.2020.562181

52. Zhang Y, Lei CW, Chen X, Yao TG, Yu JW, Hu WL, et al. Characterization of IncC Plasmids in Enterobacterales of Food-Producing Animals Originating From China. Front Microbiol. 2020;11:580960.

53. Carattoli A. Resistance Plasmid Families in Enterobacteriaceae. Antimicrob Agents Chemother. 2009;53(6):2227–38.

54. Rozwandowicz M, Brouwer MSM, Fischer J, Wagenaar JA, Gonzalez-Zorn B, Guerra B, et al. Plasmids Carrying Antimicrobial Resistance Genes in Enterobacteriaceae. Journal of Antimicrobial Chemotherapy. 2018;73(5):1121–37.

55. Schroll C, Huang K, Ahmed S, Kristensen BM, Pors SE, Jelsbak L, et al. The SPI-19 encoded type-six secretion-systems (T6SS) of *Salmonella enterica* serovars Gallinarum and Dublin play different roles during infection. Veterinary Microbiology. 2019;230:23–31.

56. Chattaway MA, Langridge GC, Wain J. *Salmonella* Nomenclature in the Genomic Era: A Time for Change. Sci Rep. 2021;11(1):7494.

57. Hu X, Chen Z, Xiong K, Wang J, Rao X, Cong Y. Vi Capsular Polysaccharide: Synthesis, Virulence, and Application. Critical Reviews in Microbiology. 2017;43(4):440–52.

58. Janis C, Grant AJ, McKinley TJ, Morgan FJE, John VF, Houghton J, et al. *In Vivo* Regulation of the Vi Antigen in *Salmonella* and Induction of Immune Responses with an *in vivo*-inducible Promoter. Infect Immun. 2011;79(6):2481–8.

59. Clare B. Inflammasome activation by *Salmonella*. Current Opinion in Microbiology. 2021 Dec 1;64:27–32.

60. Carden S, Okoro C, Dougan G, Monack D. Non-typhoidal *Salmonella* Typhimurium ST313 Isolates that Cause Bacteremia in Humans Stimulate Less Inflammasome Activation than ST19 Isolates Associated with Gastroenteritis. Pathogens and Disease. 2015;73(4):ftu023.

61. Souvorov A, Agarwala R, Lipman DJ. SKESA: Strategic K-mer Extension for Scrupulous Assemblies. Genome Biology. 2018;19(1):153.

62. Wood DE, Salzberg SL. Kraken: ultrafast metagenomic sequence classification using exact alignments. Genome Biology. 2014 Mar 3;15(3):R46.

63. Yoshida CE, Kruczkiewicz P, Laing CR, Lingohr EJ, Gannon VPJ, Nash JHE, et al. The *Salmonella In Silico* Typing Resource (SISTR): An Open Web-accessible Tool for Rapidly Typing and Subtyping Draft *Salmonella* Genome Assemblies. PLoS One. 2016;11(1):e0147101.

64. Hunt M, Mather AE, Sánchez-Busó L, Page AJ, Parkhill J, Keane JA, et al. ARIBA: Rapid Antimicrobial Resistance Genotyping Directly from Sequencing Reads. Microb Genom. 2017;3(10). Available from: https://www.ncbi.nlm.nih.gov/pmc/articles/PMC5695208/

65. Arndt D, Grant JR, Marcu A, Sajed T, Pon A, Liang Y, et al. PHASTER: a better, faster version of the PHAST phage search tool. Nucleic Acids Res. 2016 Jul 8;44(Web Server issue):W16–21.

66. Nguyen LT, Schmidt HA, von Haeseler A, Minh BQ. IQ-TREE: A Fast and Effective Stochastic Algorithm for Estimating Maximum-Likelihood Phylogenies. Mol Biol Evol. 2015 Jan 1;32(1):268–74.

67. Minh BQ, Nguyen MAT, von Haeseler A. Ultrafast Approximation for Phylogenetic Bootstrap. Mol Biol Evol. 2013 May 1;30(5):1188–95.

68. Yu G, Smith DK, Zhu H, Guan Y, Lam TTY. *ggtree*: An R Package for Visualization and Annotation of Phylogenetic Trees with their Covariates and other Associated Data. Methods in Ecology and Evolution. 2017;8(1):28–36.

69. Tonkin-Hill G, Lees JA, Bentley SD, Frost SDW, Corander J. RhierBAPS: An R Implementation of the Population Clustering Algorithm hierBAPS. Wellcome Open Res. 2018;3:93.

70. Feldgarden M, Brover V, Haft DH, Prasad AB, Slotta DJ, Tolstoy I, et al. Using the NCBI AMRFinder Tool to Determine Antimicrobial Resistance Genotype-Phenotype Correlations Within a Collection of NARMS Isolates. bioRxiv. 2019;550707.

71. Carattoli A, Zankari E, García-Fernández A, Larsen MV, Lund O, Villa L, et al. In Silico Detection and Typing of Plasmids using PlasmidFinder and Plasmid Multilocus Sequence Typing. Antimicrobial Agents and Chemotherapy. 2014 Jul 1;58(7):3895–903.

72. Csardi G, Nepusz T. The igraph software package for complex network research. InterJournal. 2006; Complex Systems:1695.

73. Chen L, Zheng D, Liu B, Yang J, Jin Q. VFDB 2016: Hierarchical and Refined Dataset for Big Data Analysis—10 Years On. Nucleic Acids Res. 2016;44:D694–7.

74. Mansour MN, Yaghi J, El Khoury A, Felten A, Mistou MY, Atoui A, et al. Prediction of *Salmonella* Serovars Isolated from Clinical and Food Matrices in Lebanon and Genomic-based Investigation Focusing on Enteritidis Serovar. International Journal of Food Microbiology. 2020;333:108831.

75. Suez J, Porwollik S, Dagan A, Marzel A, Schorr YI, Desai PT, et al. Virulence Gene Profiling and Pathogenicity Characterization of Non-Typhoidal *Salmonella* Accounted for Invasive Disease in Humans. PLoS One. 2013 Mar 7;8(3):e58449.

76. Sévellec Y, Vignaud ML, Granier SA, Lailler R, Feurer C, Le Hello S, et al. Polyphyletic Nature of *Salmonella enterica* Serotype Derby and Lineage-Specific Host-Association Revealed by Genome-Wide Analysis. Frontiers in Microbiology. 2018;9:891.

77. Hayward MR, Jansen VA, Woodward MJ. Comparative Genomics of *Salmonella enterica* serovars Derby and Mbandaka, Two Prevalent Serovars Associated with Different Livestock Species in the UK. BMC Genomics. 2013;14:365.

78. Kérouanton A, Hirchaud E, Rose V, Esnault E, Naquin D, Denis M. First Complete Genome Sequence of a *Salmonella enterica* subsp. *enterica* Serovar Derby Strain Associated with Pork in France. Genome Announc. 2015;3(4):e00853-15.

79. Suchard MA, Lemey P, Baele G, Ayres DL, Drummond AJ, Rambaut A. Bayesian Phylogenetic and Phylodynamic Data Integration Using BEAST 1.10. Virus Evolution. 2018;4(1). Available from: https://doi.org/10.1093/ve/vey016

80. Croucher NJ, Page AJ, Connor TR, Delaney AJ, Keane JA, Bentley SD, et al. Rapid Phylogenetic Analysis of Large Samples of Recombinant Bacterial Whole Genome Sequences Using Gubbins. Nucleic Acids Research. 2015;43(3):e15.

81. Rambaut A, Lam TT, Max Carvalho L, Pybus OG. Exploring the Temporal Structure of Heterochronous Sequences using TempEst (formerly Path-O-Gen). Virus Evol. 2016;2(1):vew007.

82. Duchene S, Lemey P, Stadler T, Ho SYW, Duchene DA, Dhanasekaran V, et al. Bayesian Evaluation of Temporal Signal in Measurably Evolving Populations. Molecular Biology and Evolution. 2020;37(11):3363–79.

83. Ayres DL, Darling A, Zwickl DJ, Beerli P, Holder MT, Lewis PO, et al. BEAGLE: An Application Programming Interface and High-Performance Computing Library for Statistical Phylogenetics. Systematic Biology. 2012 Jan 1;61(1):170–3.

84. Chen S, Zhou Y, Chen Y, Gu J. fastp: an ultra-fast all-in-one FASTQ preprocessor. Bioinformatics. 2018 Sep 1;34(17):i884–90.

85. Wick RR, Judd LM, Cerdeira LT, Hawkey J, Méric G, Vezina B, et al. Trycycler: Consensus Long-read Assemblies for Bacterial Genomes. Genome Biology. 2021 Sep 14;22(1):266.

86. Wick RR, Judd LM, Gorrie CL, Holt KE. Unicycler: Resolving Bacterial Genome Assemblies From Short and Long Sequencing Reads. PLOS Computational Biology. 2017;13(6):e1005595.

87. Wick RR, Schultz MB, Zobel J, Holt KE. Bandage: interactive visualization of de novo genome assemblies. Bioinformatics. 2015 Oct 15;31(20):3350–2.

88. Seemann T. Prokka: Rapid Prokaryotic Genome Annotation. Bioinformatics (Oxford, England). 2014;30(14):2068–9.

89. Alikhan NF, Petty NK, Ben Zakour NL, Beatson SA. BLAST Ring Image Generator (BRIG): Simple Prokaryote Genome Comparisons. BMC Genomics. 2011;12(1):402.

90. Carattoli A, Hasman H. PlasmidFinder and *In Silico* pMLST: Identification and Typing of Plasmid Replicons in Whole-Genome Sequencing (WGS). Methods in Molecular Biology (Clifton, NJ). 2020;2075:285.

91. Robertson J, Nash JHEY. MOB-suite: Software Tools for Clustering, Reconstruction and Typing of Plasmids from Draft Assemblies. Microbial Genomics. 2018;4(8):e000206.

92. Sullivan MJ, Petty NK, Beatson SA. Easyfig: a genome comparison visualizer. Bioinformatics. 2011 Apr 1;27(7):1009–10.

93. Tonkin-Hill G, MacAlasdair N, Ruis C, Weimann A, Horesh G, Lees JA, et al. Producing Polished Prokaryotic Pangenomes with the Panaroo Pipeline. Genome Biology. 2020;21(1):180.

ACKNOWLEDGEMENTS

We thank all staff members of the Enterics and MDDI section at the Microbiological Diagnostic Unit Public Health Laboratory (MDU PHL) for their technical assistance. We would also like to thank Jake Lacey for his assistance uploading the reads to NCBI. The BEAST analysis for this paper was undertaken using the LIEF HPC-GPGPU Facility hosted at the University of Melbourne. This Facility was established with the assistance of LIEF Grant LE170100200.

AUTHOR INFORMATION

These authors contributed equally: Deborah A Williamson, Jaclyn S Pearson, Danielle J Ingle

Authors and Affiliations

Department of Microbiology and Immunology, The University of Melbourne at The Peter Doherty Institute for Infection and Immunity, Melbourne, Victoria, Australia.

Cheryll M Sia, Benjamin P Howden, Danielle J Ingle

Centre for Innate Immunity and Infectious Diseases, Hudson Institute of Medical Research, Clayton, Melbourne, VIC, Australia.

Rebecca Ambrose, Jaclyn S Pearson

971 **Department of Infectious Diseases, The University of Melbourne at the Peter Doherty**
972 **Institute for Infection and Immunity, Melbourne, VIC, Australia.**
973 Deborah A Williamson
974
975 **Microbiological Diagnostic Unit Public Health Laboratory, Department of Microbiology**
976 **& Immunology, The University of Melbourne at The Peter Doherty Institute for Infection**
977 **and Immunity, Melbourne, Victoria, Australia.**
978 Mary Valcanis, Patiyan Andersson, Susan A Ballard, Benjamin P Howden
979
980 **Department of Microbiology, Monash University, Clayton, Victoria, Australia.**
981 Jaclyn S Pearson
982
983 **School of Medicine, University of St Andrews, St Andrews, Fife, Scotland.**
984 Jaclyn S Pearson
985
986 **Contributions**
987 Study design and oversight: CMS, RA, DAW, JSP, DJI. Isolate collection and metadata: MV,
988 PA, SAB, BJP. Performed wet lab experiments: RA, JSP. Data analysis: CMS, RA, JSP, DJI.
989 Manuscript writing: CMS, RA, DAW, JSP, DJI. All authors contributed to manuscript editing.
990
991 **ETHICS DECLARATIONS**
992 **Competing interests**
993 The authors declare no competing financial interests.
994
995

996 **Figures and Tables**

997

998 **Figure 1. Overview of *S.* Dublin genomes in study**

999 Geographical distribution and clonal relationship of 1,303 *S.* Dublin genomes in the study. A)
1000 Number of *S*. Dublin genomes according to geographical region and time interval of collection.
1001 B) Distribution of human, animal and food *S*. Dublin genomes collected over time. C)
1002 Distribution of *S*. Dublin sequence types (ST) from each region. Each coloured circle correlates
1003 to an ST. Circles in green indicate no ST was identified. D) Unrooted phylogenetic tree of 1,303
1004 *S.* Dublin genomes. Two main lineages of ST74 (n=8) and ST10 (n=1,295) shown in blue and
1005 pink respectively. E) Relatedness of known sequence types (STs) to ST10. The nodes are
1006 labelled with the ST and the branch lengths are indicative of the number of dissimilar locus
1007 variants to ST10.

1008

1009

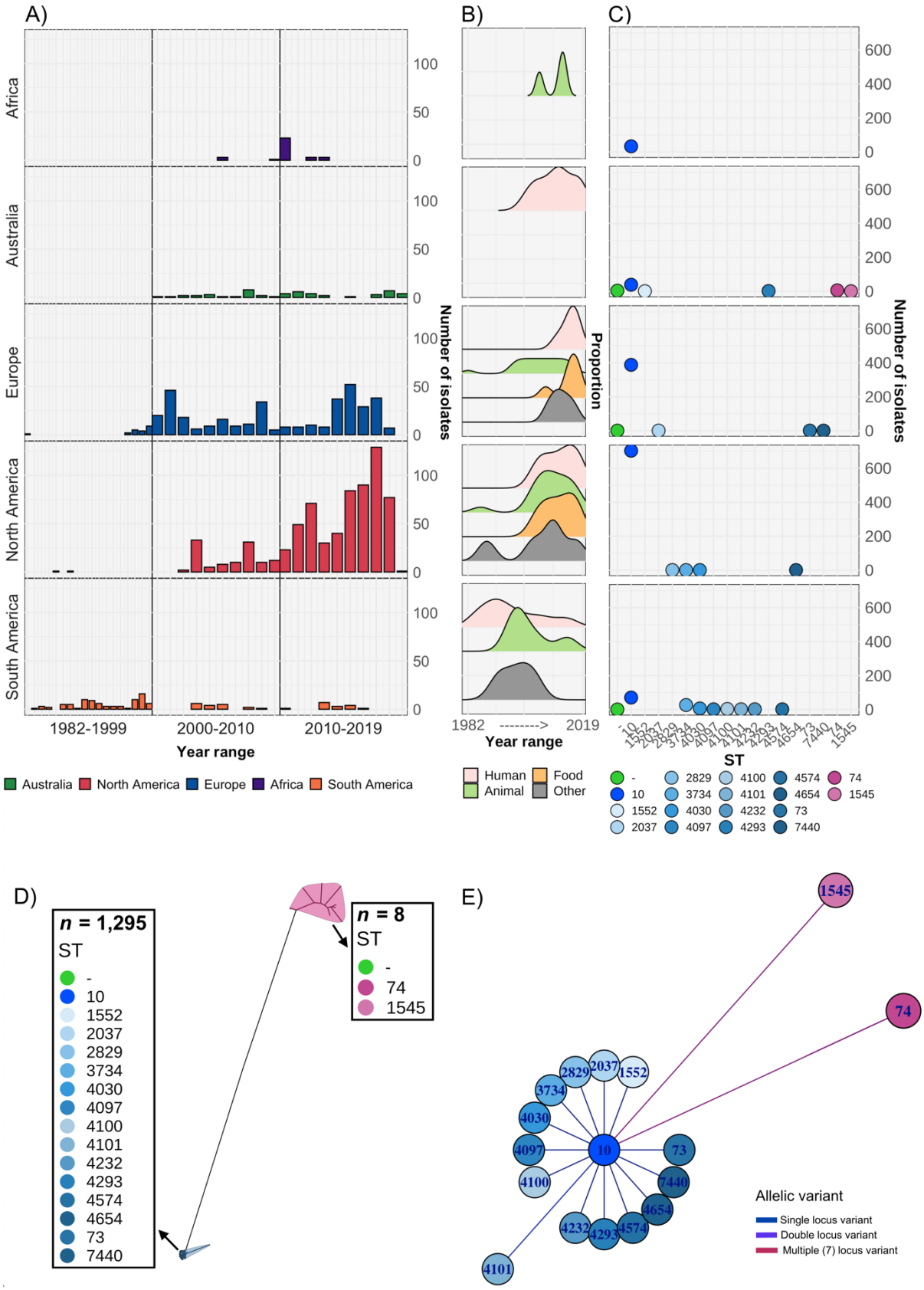

1010

1011

1012

1013 **Figure 2. Estimation of divergence time**

1014 Maximum clade credibility (MCC) tree of the 667 *S.* Dublin ST10 genomes. The time in years

1015 is shown on the x-axis. From left to right, the coloured heatmaps refer to the region of origin,

1016 the susceptibility profile, the BAPs clade, and the presence of IncC and IncN plasmid types.

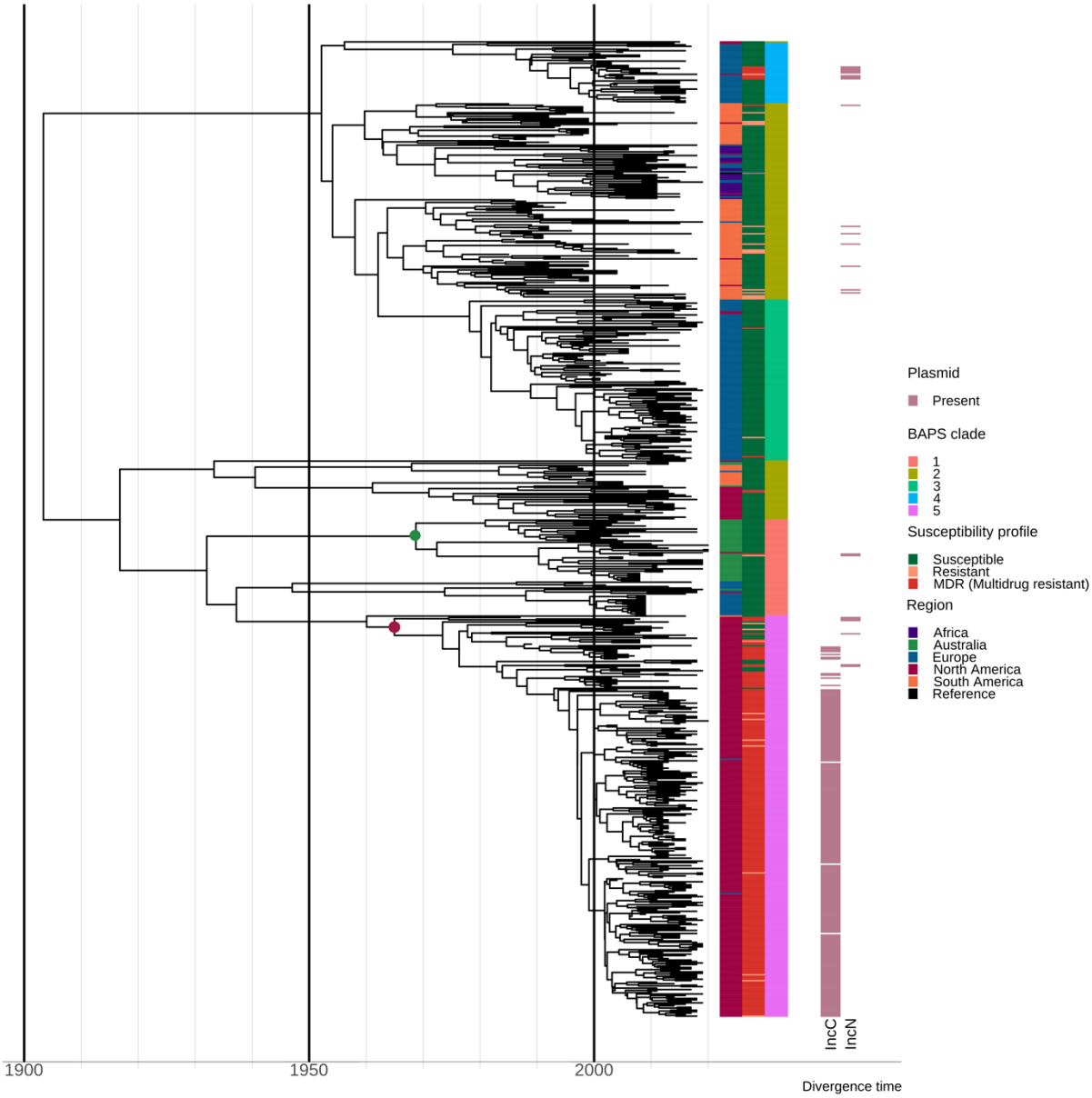

1017

1018

1019

1020

1021

Figure 3. Resistance profiles of *S.* Dublin genomes

Observed resistance profiles of *S.* Dublin genomes spanning three-time intervals for each region. A) Frequency of susceptible and resistant *S.* Dublin genomes from each time period B) Antimicrobial resistance profiles observed spanning three time periods. The colour of the circle corresponds to an antimicrobial class, while the height is relative to the number of genomes. C) Heavy metal and biocide resistance profiles observed. The colour of the circle corresponds to its respective heavy metal/biocide class, while the height is relative to the number of genomes.

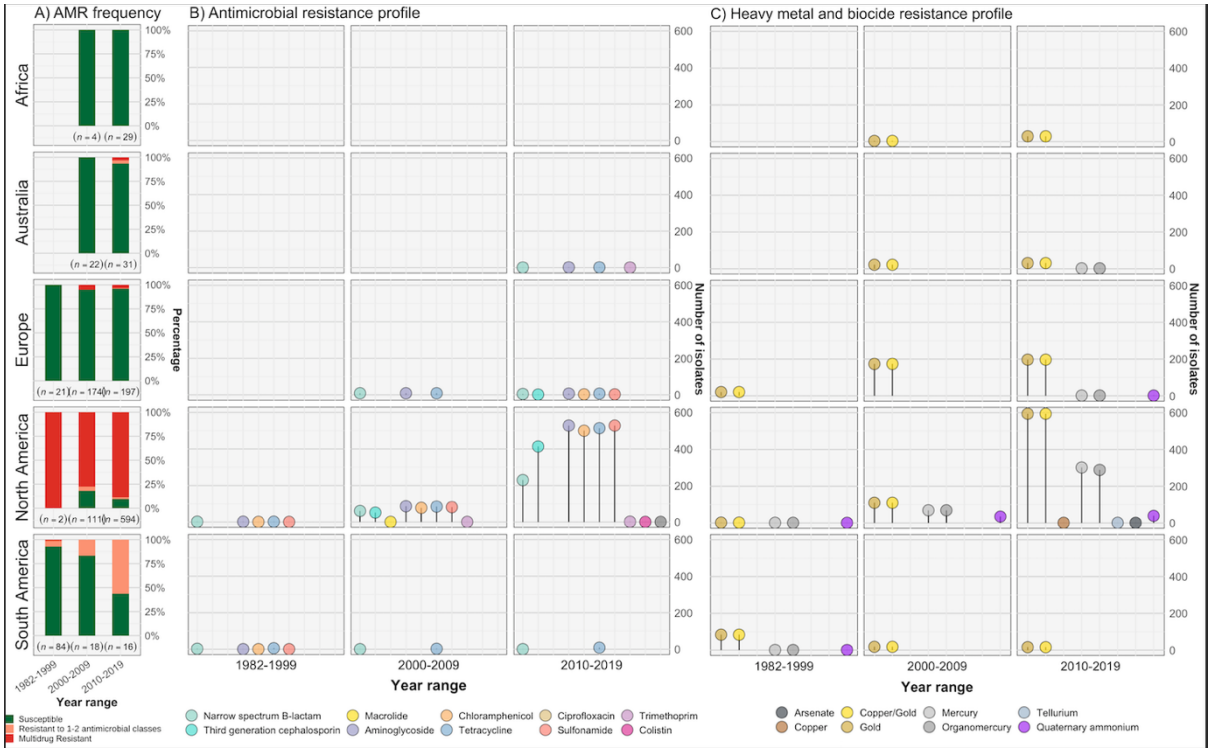

1032 **Figure 4. Invasive factors associated with *S.* Dublin genomes**

1033 Correlation of *Salmonella* pathogenicity islands (SPIs) to *S.* Dublin's invasiveness. A)
1034 Validation of the likelihood of invasiveness prediction tool using a variety of publicly available
1035 genomes consisting of non-invasive and invasive *Salmonella* serovars (Supplementary Table
1036 8). B) The correlation of index scores to the source and its sequence type based on the region.
1037 * indicates a statistically significant p-value between the index scores of two sources. C)
1038 Chromosomal assemblies of ST10 (blue) and ST74 (pink) genomes aligned to *S.* Dublin
1039 chromosomal reference CT_02021853 (CP001144.1) with a lower limit of 80% identity D)
1040 Aligned sequence of SPI-6 region of an ST10, AUSMDU00056868, and an ST74,
1041 AUSMDU00016676, in comparison to SPI-6 region of reference CT_02021853. E) Aligned
1042 sequence of SPI-19 region of an ST10, AUSMDU00056868, and an ST74,
1043 AUSMDU00016676 in comparison to SPI-19 region of reference CT_02021853.

1044 SPI, *Salmonella* pathogenicity island.

1045

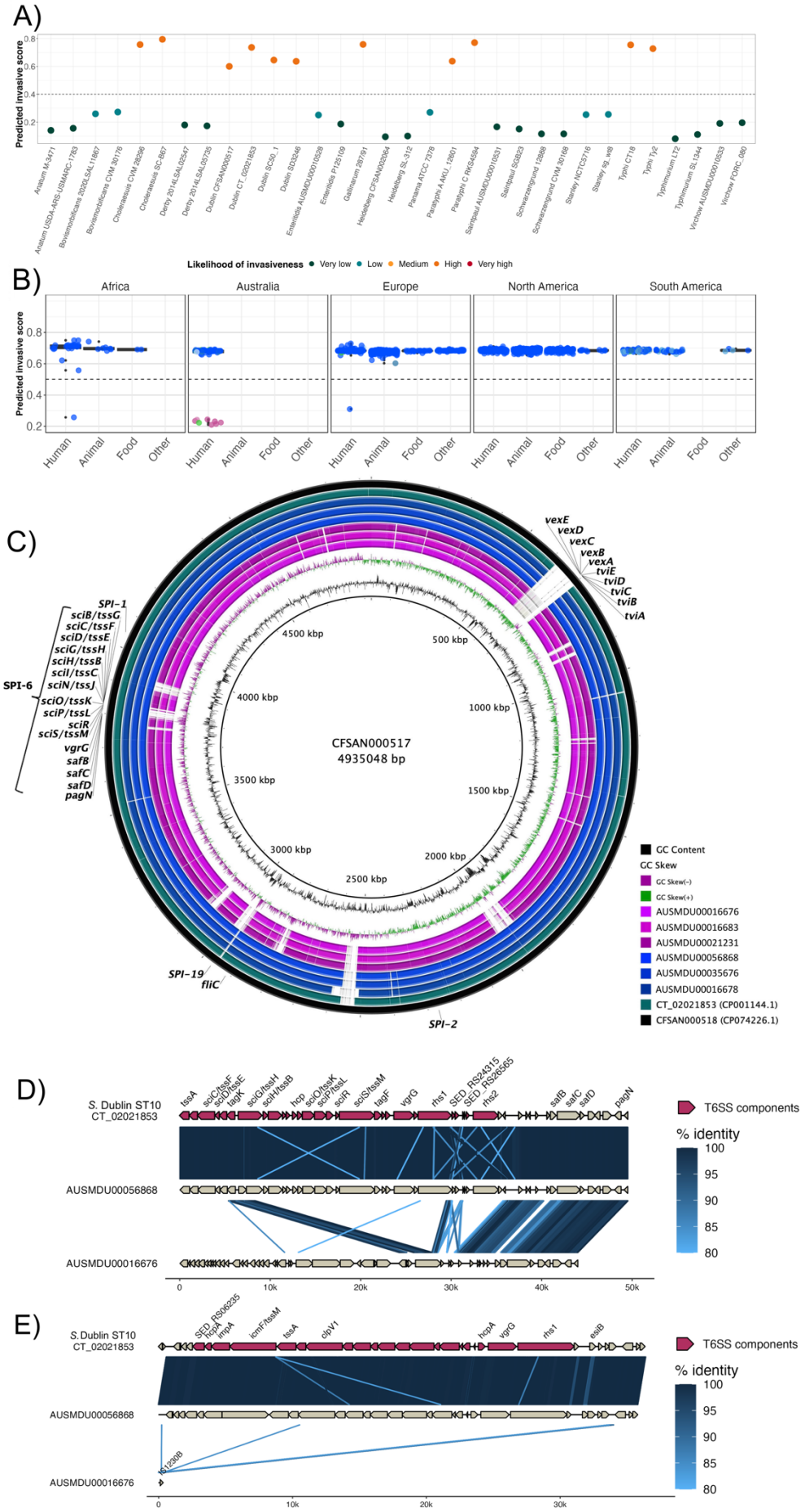
A)
Predicted invasive score
Likelihood of invasiveness
Very low
Low
Medium
High
Very high
B)
Africa
Australia
Europe
North America
South America
Predicted invasive score
Human
Animal
Food
Other
C)
CFSAN000517
4935048 bp
500 kbp
1000 kbp
1500 kbp
2000 kbp
2500 kbp
3000 kbp
3500 kbp
4000 kbp
4500 kbp
SPI-1
sciB/tssG
sciC/tssF
sciD/tssE
sciG/tssH
sciH/tssB
sciI/tssC
sciN/tssJ
SPI-6
sciO/tssK
sciP/tssL
sciR
sciS/tssM
vgrG
safB
safC
safD
pagN
vexE
vexD
vexC
vexB
vexA
tviE
tviD
tviC
tviB
tviA
SPI-19
fliC
SPI-2
GC Content
GC Skew
GC Skew(-)
GC Skew(+)
AUSMDU00016676
AUSMDU00016683
AUSMDU00021231
AUSMDU00056868
AUSMDU00035676
AUSMDU00016678
CT_02021853 (CP001144.1)
CFSAN000518 (CP074226.1)
D)
S. Dublin ST10
CT_02021853
AUSMDU00056868
AUSMDU00016676
T6SS components
% identity
100
95
90
85
80
0
10k
20k
30k
40k
50k
E)
S. Dublin ST10
CT_02021853
AUSMDU00056868
AUSMDU00016676
T6SS components
% identity
100
95
90
85
80
0
10k
20k
30k

1046

1047

1048 **Figure 5. *S.* Dublin ST74 isolates demonstrate increased intracellular replication in**
1049 **human macrophages over ST10 isolates**

1050 Differentiated THP-1 (human monocyte) cells were infected at an MOI:10 with selected ST10
1051 and ST74 *S.* Dublin isolates. **A, B)** THP-1 cells were lysed, and intracellular bacteria
1052 enumerated as fold change in replication and **C-F)** CFU/well at time 0, 3, 9 and 24 hpi. For **A)**,
1053 each measurement at times 3, 9 and 24 hpi represents the fold change in CFU/well compared
1054 to 0 hpi, the start of infection, recorded as a biological replicate (performed in technical
1055 triplicate), with error bars indicating ± 1 standard deviation of n = 3 biological replicates. For
1056 **C-D**), each dot represents CFU/well of a biological replicate (performed in technical triplicate),
1057 with error bars indicating ± 1 standard deviation of n = 3 biological replicates. Statistical
1058 significance was determined by nested student's t-test. MOI, multiplicity of infection, hpi,
1059 hours post-infection, CFU, colony-forming units, FC, fold-change.

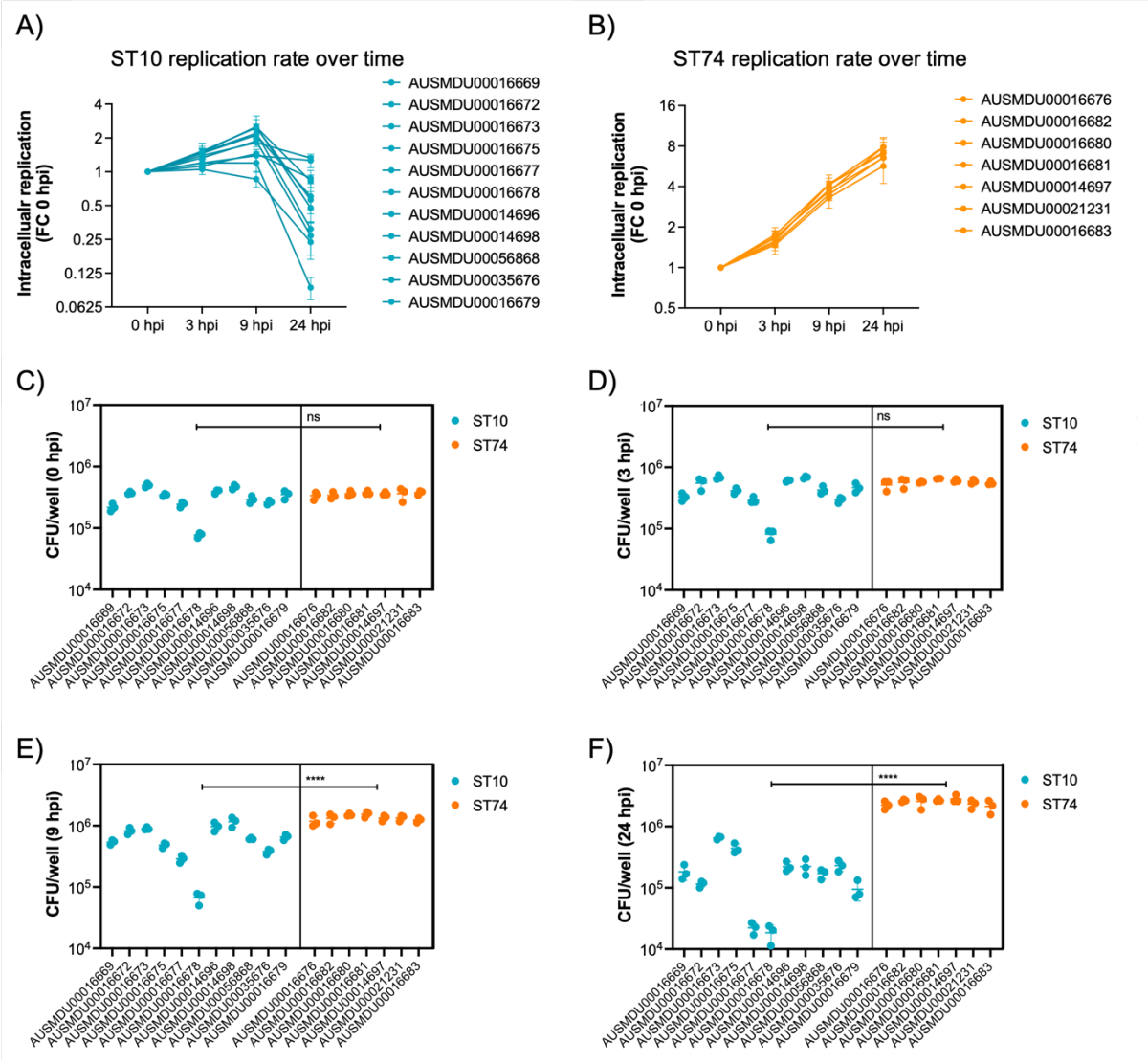

Figure 6. *S.* Dublin ST74 isolates induce comparable cytotoxicity to ST10 isolates in human macrophages, despite increased intracellular growth

A-C) Cell supernatants were assayed for LDH as a measure of cytopathic effects of infection, and % cytotoxicity was calculated by comparison with 100% lysed uninfected control cells. Samples were collected from THP-1 cells at 3, 9 and 24 hpi. Each point represents the % cytotoxicity of a biological replicate (performed in technical triplicate), with error bars indicating ± 1 standard deviation of n = 3 biological replicates. Statistical significance was determined by nested student's t-test. **D)** IL-1ß secretion from THP-1 cells infected for 9 hours with *S.* Dublin isolates. Error bars indicate ± 1 standard deviation of n = 3 biological replicates

1071 and statistical significance determined by student's t-test **E)** Immunoblot of cleaved IL-1ß
1072 (Asp166) in THP-1 cell lysates infected with *S.* Typhimurium reference strain SL1344,
1073 *S.* Dublin ST10 (AUSMDU00016673), or *S.* Dublin ST74 (AUSMDU00016682) over 0, 3, 8
1074 and 24 hours. **F)** PCA plot comparing replication rate, % cytotoxicity and IL-1β secretion from
1075 THP-1 cells infected with *S.*Dublin isolates at 9 hpi. Each dot represents each biological
1076 replicate of three (averaged from three technical replicates). .MOI, multiplicity of infection,
1077 hpi, hours post-infection, CFU, colony-forming units, LDH, lactate dehydrogenase.

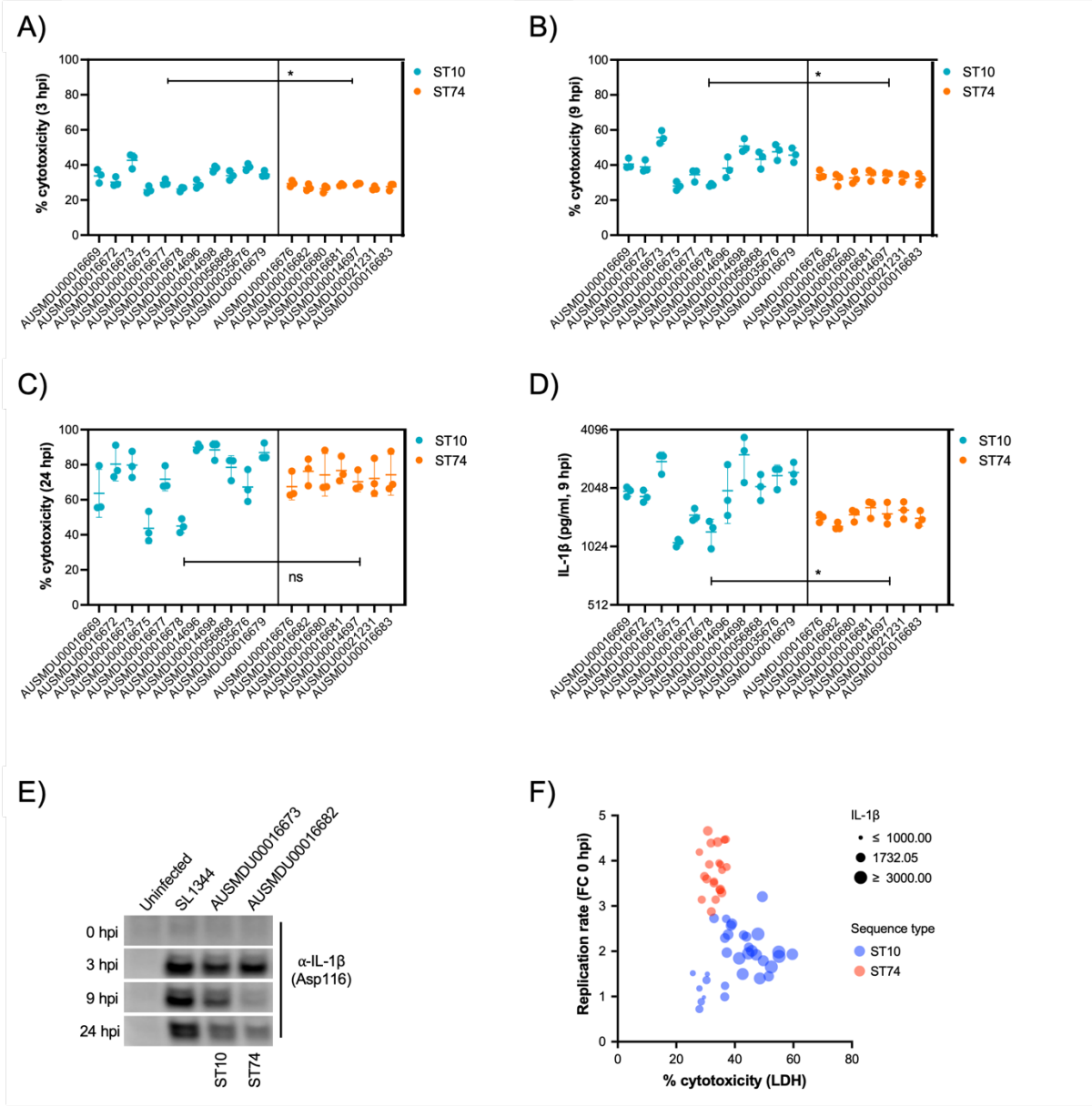

1078